AFRL-RI-RS-TR-2024-040

MULTI-DISCIPLINARY OPTIMIZATION FOR PACKAGING (MDOP)

RAYTHEON TECHNOLOGIES RESEARCH CENTER

APRIL 2024

FINAL TECHNICAL REPORT

APPROVED FOR PUBLIC RELEASE; DISTRIBUTION UNLIMITED

STINFO COPY

AIR FORCE RESEARCH LABORATORY
INFORMATION DIRECTORATE

■ **AIR FORCE MATERIEL COMMAND** ■ **UNITED STATES AIR FORCE** ■ **ROME, NY 13441**

NOTICE AND SIGNATURE PAGE

Using Government drawings, specifications, or other data included in this document for any purpose other than Government procurement does not in any way obligate the U.S. Government. The fact that the Government formulated or supplied the drawings, specifications, or other data does not license the holder or any other person or corporation; or convey any rights or permission to manufacture, use, or sell any patented invention that may relate to them.

This report was cleared for public release by the AFRL Wright-Patterson AFB Public Affairs Office and is available to the general public, including foreign nationals. Copies may be obtained from the Defense Technical Information Center (DTIC) (http://www.dtic.mil).

AFRL-RI-RS-TR-2024-040 HAS BEEN REVIEWED AND IS APPROVED FOR PUBLICATION IN ACCORDANCE WITH ASSIGNED DISTRIBUTION STATEMENT.

FOR THE CHIEF ENGINEER:

/ S /
STEVEN L. DRAGER
Work Unit Manager

/ S /
NICK P. KOWALCHUK
RIT Chief Engineer
Computing & Communications Division
Information Directorate

This report is published in the interest of scientific and technical information exchange, and its publication does not constitute the Government's approval or disapproval of its ideas or findings.

REPORT DOCUMENTATION PAGE

PLEASE DO NOT RETURN YOUR FORM TO THE ABOVE ORGANIZATION.

1. REPORT DATE	2. REPORT TYPE	3. DATES COVERED	
		START DATE	END DATE
APRIL 2024	FINAL TECHNICAL REPORT	FEBRUARY 2023	DECEMBER 2023

4. TITLE AND SUBTITLE

MULTI-DISCIPLINARY OPTIMIZATION FOR PACKAGING (MDOP)

5a. CONTRACT NUMBER	5b. GRANT NUMBER	5c. PROGRAM ELEMENT NUMBER
FA8750-23-C-0501	N/A	62303E
5d. PROJECT NUMBER	**5e. TASK NUMBER**	**5f. WORK UNIT NUMBER**
N/A	N/A	R3E1

6. AUTHOR(S)

Larry E. Zeidner, Joseph E. Turney, Raphael Mandel, Shane E. Haydt, Horea Lies, Mohammad Behzadi, Peter Zaffetti, James T. Allison, Nathan M. Dunfield, Nancy Amato, Chad Peterson, Isaac B. Love, Stav Ashur, Marco Morales Aguirre

7. PERFORMING ORGANIZATION NAME(S) AND ADDRESS(ES)

Raytheon Tech Research Center
411 Silver Lane
East Hartford, CT 06118

8.PERFORMING ORGANIZATIONREPORT NUMBER

9. SPONSORING/MONITORING AGENCY NAME(S) AND ADDRESS(ES)

DARPA
675 North Randolph Street
Arlington, VA 22203-2114

Air Force Research Laboratory/RITA
525 Brooks Road
Rome NY 13441-4505

10.SPONSOR/MONITOR 'S ACRONYM(S)

AFRL/RI & DARPA

11.SPONSOR/MONITOR'S REPORT NUMBER(S)

AFRL-RI-RS-TR-2024-040

12. DISTRIBUTION/AVAILABILITY STATEMENT

Approved for Public Release; Distribution Unlimited. PA# AFRL-2024-2043 / AFRL-2024-0448
Date Cleared: 22 APR 2024

13. SUPPLEMENTARY NOTES

14. ABSTRACT

This report documents research conducted under the Defense Advanced Research Projects Agency (DARPA) Multi-Disciplinary Optimization for Packaging (MDOP) seedling effort. The goal of developing a mathematical framework employing technologies that allow automated, optimal packaging design of complex Cyber-Physical Systems (CPS) was to distill DARPA-hard technical challenge(s) that must be solved to enable an MDOP capability, with Department of Defense (DoD) wide applicability, enabling the Aerospace and Defense Industry to develop substantially more functionally dense complex CPS that the DoD critically needs. This report defines the overall MDOP problem, the scoped DARPA Seedling MDOP problem, methods, results, and conclusions, including the DARPA-hard technical challenge(s) required to develop an MDOP capability, applicable across DoD, that would substantially improve the requirements that systems can achieve.

15. SUBJECT TERMS

Complex Cyber-Physical Systems, Multi-Disciplinary Optimization, Mathematical Framework, Maximal Disjoint Ball Decomposition, Topological Partitioning

16. SECURITY CLASSIFICATION OF:			17. LIMITATION OF ABSTRACT	18. NUMBER OF PAGES
a. REPORT	b. ABSTRACT	C. THIS PAGE		
U	U	U	SAR	59

19a. NAME OF RESPONSIBLE PERSON	19b. PHONE NUMBER *(Include area code)*
STEVEN L. DRAGER	N/A

STANDARD FORM 298 (REV. 5/2020)
Prescribed by ANSI Std. Z39.18

TABLE OF CONTENTS

List of Figures ii
List of Tables v
1.0 SUMMARY 1
2.0 INTRODUCTION 2
2.1 Problem Definition 2
2.2 Objectives 3
2.3 Related Prior Work 4
2.4 Key Research Questions (RQ) 4
2.5 DARPA MDOP Seedling Scoping 4
3.0 METHODS, ASSUMPTIONS, AND PROCEDURES 6
3.1 Methods 6
3.1.1 Approach 6
3.2 Assumptions 6
3.2.1 MDOP Computational Workflow 6
3.3 Procedures 8
3.3.1 Development of Topological Partitioning 8
3.3.2 Development of Co-Optimized Physics and Spatial Configuration 14
3.3.3 Development of Spatial Accessibility Value Metrics 18
3.3.4 Development of Co-Optimized Physics, Spatial Configuration and Accessibility 21
3.3.5 Validation 26
4.0 RESULTS AND DISCUSSION 30
4.1 MDOP Computational Workflow Demonstrated at Small Scale 30
4.1.1 Topological Partitioning Demonstrated 30
4.1.2 Co-optimization of Physics and Spatial Configuration Demonstrated 33
4.1.3 Co-optimization of Physics Spatial Configuration *and Accessibility* Demonstrated.. 34
4.2 Validation Results for Computational Workflow Elements 36
5.0 CONCLUSIONS 37
5.1 MDOP Methods Assessment 37
5.1.1 Topological Partitioning Methods Assessment Conclusions 37
5.1.2 MDBD Assessment Conclusions 38
5.1.3 Enclosure Constraint Conclusions 38
5.1.4 Interconnect Constraints 41
5.1.5 Combined Component and Interconnect Constraints and Waypoint Relocation ... 42
5.1.6 MDOP's Potential Impact on Design of DoD Systems 42
6.0 REFERENCES 48
LIST OF SYMBOLS, ABBREVIATIONS, AND ACRONYMS 49

LIST OF FIGURES

Figure 1: A notional MDOP system of components and interconnects, fitting within an enclosure, around obstacles, with ambient, component-generated, and interconnect-generated multi-physics fields, to which certain components and interconnects are sensitive, i.e., their value metrics change depending upon the fields they experience in their environment. 2

Figure 2: A notional example of components and local interconnectects allocated across a distributed set of enclosures on a vehicle, interconnected via remote interconnects through pathways. 2

Figure 3: A spatial graph of an automotive power system, illustrated topologically, in a 2D schematic including component geometry, and in a 3D geometric realization (Peddada, 2022). 4

Figure 4: A 2D MDBD geometric representation of a shape as it changes, illustrating how the representation updates only locally, with gradual, localized changes (Jiangce Chen, 2020). 4

Figure 5: Illustrations showing how components and interconnects can be resized and reshaped, within an enclosure, without colliding with any obstacles [black rectangles], one another, or the enclosure boundary. The top illustration shows how this is done correctly, while the bottom shows the most common failure modes. 5

Figure 6: The transition through 3 topological states: a) interconnect I_1 is over interconnect I_2, b) interconnects I_1 and I_2 share 3D volume, which is not a physically realizable state, and c) interconnect I_2 is over interconnect I_1. 6

Figure 7: The MDOP Topological Partitioning computational step transforms the MDOP problem from the infinite, continuous geometric-configuration design space (i), to the infinite, discrete topological design space by selecting a very small subset of spatial topologies (green circles in ii) which eliminates infinitely large "complexity cones" of undesirably complex topologies efficiently, and transforms them back to independent contiguous regions of the geometric-configuration space, that are analogous to cells within a closed-cell foam (iii). Each cell that is the target of a selected spatial topology transformed back into this space is the subject of an independent co-optimization of multi-physics-based value-metrics, spatial-compactness value metrics, and spatial accessibility value metrics. The selected cells can be optimized in parallel. 8

Figure 8: The transformations that constitute the modules of the TP computational workflow. Note that Module 4 is used to verify that all Output GRs generated by Module 3 and Module 5 preserve the Spatial Topology of the unique SGD from which they were generated. 12

Figure 9: Stochastic force-directed layout, with 3D rotation, to generate a set of 3D Geometric Realizations from which a diverse set can be selected. 12

Figure 10: A physics-based diversity metric that considers, for each 3D Geometric Realization, which components and elbows are closest to a set of physically relevant external locations. 13

Figure 11: Example: in one geometric realization, a heat-sensitive component is adjacent to a hot pipe of another system. In another geometric realization, it is near the cold heating, ventilation and air conditioning (HVAC) ducting. 14

Figure 12: 2D and 3D spatial optimization using MDBD. 15

Figure 13: An illustration of the concept of using dimensional elevation, in geometric optimization, to avoid local minima..... 16

Figure 14: An example of geometric optimization, using MDBD with dimensional elevation, to avoid local minima. (a) initial condition, (b) w/o dimension elevation, the optimization reaches a local minimum with the interconnect stuck on the torus, and (c) with dimension elevation: interconnect proceeds past torus for compact packaging..... 17

Figure 15: An example of geometric optimization, using MDBD with dimensional elevation, to avoid local minima. (a) initial condition, (b) w/o dimension elevation, the optimization reaches a local minimum with the interconnect between the blue (top right) component and the orange component stuck on the yellow component (e.g., the orange component cannot go farther down to the right to get around the yellow component because that would increase the packaging volume), and (c) with dimension elevation: orange component proceeds past yellow component for compact packaging near bottom blue component. 18

Figure 16: Snapshot of simulation video showing lower path selected due to path width. 20

Figure 17: Snapshot of simulation video showing upper path selected due to risk-weighted cost (proximity and fragility) of lower wider path exceeding the cost of the narrower upper path. 20

Figure 18: Two examples of "blocking," as an element of removal and replacement cost. Note than when the components needing frequent service, and thus frequent removal/replacement were on the top (easiest access), the cost was better, and when they were buried on the bottom, they were blocked by many other components, so the cost was worse. 21

Figure 19: A Graphics Interchange Format (GIF) showing co-optimization of spatial compactness and spatial accessibility..... 24

Figure 20: Computational profiling results of the co-optimization workflow shows spatial accessibility scaling poorly, and the gradient (which is being replaced in Task4). 25

Figure 21: An RTX physics-sizing model has been integrated to the spatial model in a modular fashion within OpenMDAO. The optimization problem has been fully flattened so that the OpenMDAO optimizer provides a design vector to each model (physics, spatial). The physics and spatial models are called independently; coupling is done entirely via constraints, other than the physics model passing the updated component and interconnect geometry to the spatial model for configuration. 27

Figure 22: Specification of interconnect spatial model: N straight segments, connecting N+1 waypoints, with each segment populated with overlap-ping spheres. 28

Figure 23: In the left geometric realization, the heat-sensitive component is sandwiched between two hot components. In the right geometric realization, it is far away from both. 30

Figure 24: Module 5 Examples. NOTE: This process is NOT random -- it preserves the Unique Spatial Topology. 31

Figure 25: The Topological Partitioning (TP) computational workflow applied to 2 examples.. 31

Figure 26: Computational Workflow of the MDOP Co-Optimization. 34

Figure 27: GIF of co-optimization of spatial configuration and spatial accessibility..... 35

Figure 28: GIF of co-optimization of physics, spatial configuration, and spatial accessibility.... 35

Figure 29: GIF (left) of Spiral1 co-optimization with single distance constraint shows poor stability. The histogram (right) shows that few optimizations found global optimum, while most got stuck on a local minimum. 39

Figure 30: A single distance constraint is a poor representation of the component's spatial relationship to the enclosure boundary. In this case, the single constraint doesn't support reasoning because each of the component's corners has a different relationship with the enclosure boundary. 40

Figure 31: GIF (left) of Spiral1 co-optimization with distance constraints from each component sphere to enclosure boundary has better stability. Histogram (right) shows that some optimizations found the global optimum, while many got stuck on a local minimum..... 40

Figure 32: The distance constraint derivatives for each of these 3 component corners to the enclosure boundary do a better job of capturing and supporting reasoning about the component's spatial relationship with the enclosure boundary and how to increase component size while still fitting within the enclosure. 41

Figure 33: GIF of Spiral1.5 co-optimization of an interconnect and its optimum solution..... 42

Figure 34: DoD systems that CAN'T be developed today due to packaging challenges. 43

Figure 35: Multi-region packaging allocates components across a variety of available volumes in different regions within a system, and incurs weight, cost, losses, and accessibility impacts due to routing interconnects between those volumes. 45

Figure 36: Components must be able to be resized/reshaped, during co-optimization, to optimize physics-based system value metrics..... 45

Figure 37: More-complex and flexible types of interconnects that must be addressed for applicability across a wide range of DoD systems. 46

Figure 38: An integrated scalable solution is required to get MDOP from the $O(3^n)$ curve onto the O(n log n) curve. This is needed to achieve 400,000 times speedup, which is required to achieve the most aggressive DoD requirements. 47

LIST OF TABLES

Table 1: Mathematical constructs involved in the Topological-Partitioning computational workflow, and the information that they encode. 10

Table 2: The transformations between constructs used in the TP computational workflow. 11

Table 3: Computational Profiling of Co-optimization 33

1.0 SUMMARY

This Final Technical Report documents the research conducted under this Defense Advanced Research Projects Agency (DARPA) Multi-Disciplinary Optimization for Packaging (MDOP) Seedling. The goal of developing a mathematical framework employing technologies that allow automated, optimal packaging design of complex Cyber Physical Systems (CPS) was to distill the DARPA-hard technical challenge(s) that must be solved to enable an MDOP capability, with Department of Defense (DoD)-wide applicability, that would enable the Aerospace and Defense Industry to develop substantially more functionally dense complex CPS that the DoD critically needs. This report defines the overall MDOP problem, the scoped DARPA Seedling MDOP problem, methods, results, and conclusions, including the DARPA-hard technical challenge required to develop an MDOP capability, applicable across DoD, that would substantially improve the requirements that DoD systems can achieve.

2.0 INTRODUCTION

2.1 Problem Definition

The MDOP Problem is defined as follows:

- Given a **system** consisting of:
  - A set of **components** (e.g., heat exchangers, compressors, generators) with specific three-dimensional (3D) geometry and specific geometric **ports** (**Figure 1**).
  - A set of **interconnects**: port-to-port connections (e.g., wires, wire harnesses, pipes/tubes, ducts, manifolds) connecting specific ports on various components, with specific geometric assumptions about cross-sectional two-dimensional (2D) shape, area along the trajectory, and trajectory attributes, such as maximum allowable length and minimum allowable turning radius (**Figure 1**).
  - A set of available **enclosures**: a specific set of 3D geometric volumes within which all components and **local interconnects** (that connect components packaged in the same enclosure) must fit (e.g., a set of candidate bays, cabinets, and other volumes in a vehicle, within which electric-system components may be packaged).
  - A set of **pathways**: specific 3D geometric volumes through which **remote interconnects** (that connect components packaged in different local enclosures) must be contained. (e.g., raceways along the fuselage of an aircraft, housing long wire harnesses, hydraulic lines, etc., or an engine pylon that is packed with wires, pipes, and ducts connecting the engine with the wing (**Figure 2**).
  - A set of 3D geometric **obstacles** (keep-out zones) with which NO components or interconnections can collide (e.g., other components and interconnects of another system that already live within one of the enclosures or pathways).

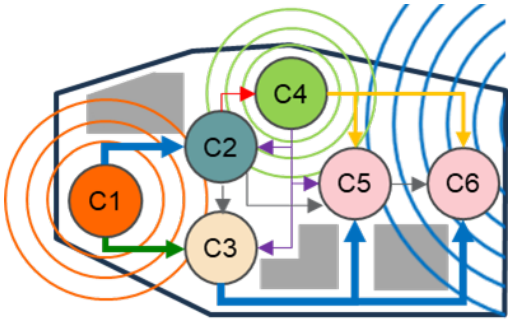

Figure 1: A notional MDOP system of components and interconnects, fitting within an enclosure, around obstacles, with ambient, component-generated, and interconnect-generated multi-physics fields, to which certain components and interconnects are sensitive, i.e., their value metrics change depending upon the fields they experience in their environment.

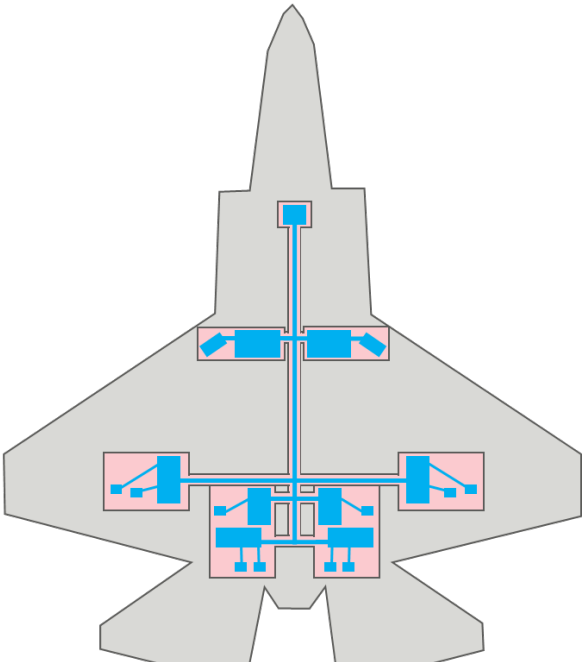

Figure 2: A notional example of components and local interconnectects allocated across a distributed set of enclosures on a vehicle, interconnected via remote interconnects through pathways.

- A set of **external Input/Output (I/O) ports**: specific 3D geometric ports to which the system must connect for I/O with the outside world, to receive system inputs and provide system outputs (e.g., a ram-air inlet, or outlet nozzle on an aircraft).
- A set of physics-based system **value metrics** (e.g., Size, Weight, Power and Cost (SWaP-C)) that are driven by the component technologies, the component tuning and sizing, and importantly, by the spatial configuration of the system (e.g., the length and resulting weight and cost of remote interconnects driven by component allocations to local enclosures, the thermal interactions driven between heat-generating and heat-sensitive components and interconnects, due to their proximity). One of the most important value metrics, due to its impact on military availability, and the cost of each life-cycle phase, is **spatial accessibility**: the ease with which the most-frequently replaced components and interconnects can be removed and replaced.

- Find 3D packaging configurations of the system with optimal value metric scores:
  - 3D position, orientation, size, and tuning of each component.
  - 3D trajectory of each interconnect from origin port to destination port.
  - System value metrics based upon this 3D packaging configuration.

  Such that the resulting configurations:
  - Are found **rapidly**: to enable co-optimization of physics and 3D spatial packaging elements of the problem, during system conceptual design, at the **large scale** of significantly **higher functional-density** DoD systems (e.g., unmanned aerial vehicles (UAVs), jet engine externals, fighter aircraft, subs, ships, and 3D heterogeneously integrated (3DHI) microelectronics).
  - Are specified at a **conceptual-design level** of detail (this is NOT the detailed-design task of placing each fastener/hanger and anti-chafe bushing).
  - Are **physically realizable**: no 3D collisions among components and among interconnects, or between them and enclosures, pathways, or obstacles.

2.2 Objectives

The objective of this DARPA MDOP Seedling was to develop MDOP, a mathematical framework employing technologies that allow automated, optimal packaging design of complex Cyber Physical Systems.

The goal of developing MDOP was intended to distill the DARPA-hard technical challenge(s) that must be solved to enable an MDOP capability, with DoD-wide applicability, that would enable the Aerospace and Defense Industry to develop substantially more functionally dense complex CPS that the DoD critically needs.

2.3 Related Prior Work

Recent advances in the National Science Foundation (NSF) sponsored Power Optimization for Electro-Thermal Systems (POETS) Consortium demonstrated that **Topological Partitioning of Spatial Graphs**, as illustrated in **Figure 3**, was possible using Yamada Polynomials in a method called Spatial Packaging of Interconnected Systems with Physical Interactions (SPI2) (Peddada S. R., 2022), (Peddada S. D., 2021).

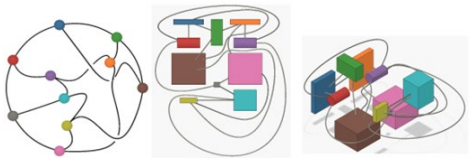

Figure 3: A spatial graph of an automotive power system, illustrated topologically, in a 2D schematic including component geometry, and in a 3D geometric realization (Peddada, 2022).

A method for geometric representation, **Maximal Disjoint Ball Decomposition (MDBD)**, is illustrated in **Figure 4**. MDBD provides a flexible and unique proxy geometric representation that implicitly parameterizes the geometric shapes in terms of collections of tangent spheres, addressing the inadequacy of current geometric representations (Jiangce Chen, 2020). The key and unique attributes of MDBD are that it:

- is dimension agnostic in the sense that it extrapolates naturally from 2D to 3D,
- describes the geometry in terms of simple spherical and hierarchical primitives that lend themselves to massive parallelization algorithms; and,
- allows the exploration of a larger subset of the design space by allowing a lifting of the problem from the original dimension of the space to higher dimensions where entanglements of the interconnections observed in the original dimensional space may not occur.

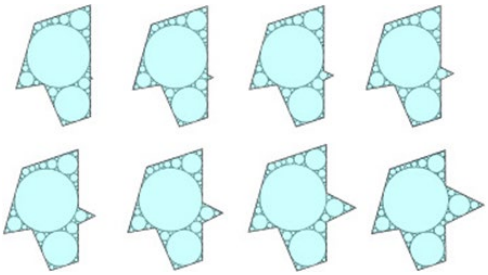

Figure 4: A 2D MDBD geometric representation of a shape as it changes, illustrating how the representation updates only locally, with gradual, localized changes (Jiangce Chen, 2020).

2.4 Key Research Questions (RQ)

- RQ1: What are the limitations of the SPI2 method for Topological Partitioning?
- RQ2: What are the limitations of the MBDB method for Geometric Representation?
- RQ3: What geometric constraints are required to enable gradient-based optimization to keep all components and interconnects inside enclosure boundaries while updating their shapes and sizes?
- RQ4: Is an End-to-End MDOP Computational Workflow Feasible?
- RQ5: Is the MDOP Computational Workflow Scalable? What are the key scalability challenges?

2.5 DARPA MDOP Seedling Scoping

The DARPA MDOP Seedling effort was scoped to a 9-month effort that would focus on the key research questions. It focused on a subset of the full MDOP problem definition:

- Given a **system** consisting of:

- Nc **components** with specific 3D geometry and specific geometric ports.
- Ni **interconnects**: port-to-port connections connecting a specific port on one component to a specific port on a second component, with specific geometric assumptions about cross-sectional 2D shape and area along the path.
- An **enclosure**: a specific 3D geometric volume within which all components and interconnects must fit, as shown in **Figure 5**, with specific 3D attachment ports, along the interior surfaces of the enclosure, to which system external interconnects must connect, to get system inputs and provide system outputs.
- A set of 3D geometric **obstacles** (keep-out zones) with which NO components or interconnections can collide (**Figure 5**).
- A set of physics-based system **value metrics** (e.g., SWaP-C) that are driven by the component technologies, the component tuning and sizing, and importantly, by the spatial configuration of the system (including spatial accessibility).

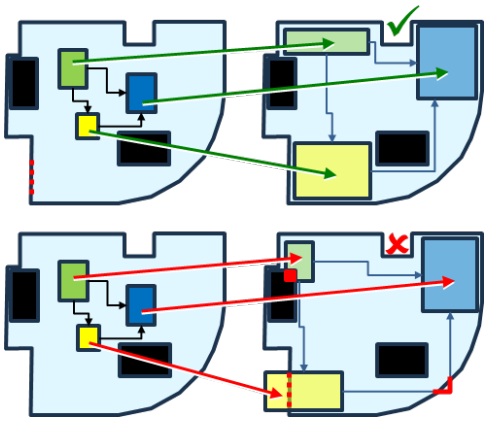

Figure 5: Illustrations showing how components and interconnects can be resized and reshaped, within an enclosure, without colliding with any obstacles [black rectangles], one another, or the enclosure boundary. The top illustration shows how this is done correctly, while the bottom shows the most common failure modes.

- Find 3D packaging configurations of the system with optimal value metric scores:
  - 3D position, orientation, size, and tuning of each component.
  - 3D trajectory of each interconnect from origin port to destination port.
  - System value metrics based upon this 3D packaging configuration.

  Such that the resulting configurations:
  - Are found **rapidly**.
  - Are specified at a **conceptual-design level** of detail.
  - Are **physically realizable**: no 3D collisions among components and among interconnects, or between them and enclosures, or obstacles.

3.0 METHODS, ASSUMPTIONS, AND PROCEDURES

3.1 Methods

3.1.1 Approach

The approach to develop a proof-of-concept MDOP capability was to leverage advances under the NSF POETS Consortium and use Topological Partitioning (TP) to find a diverse set of topological configurations which could each be geometrically optimized in parallel.

The idea was based on the observation that when two interconnections (I_1 and I_2) transition, in an optimization solver that is trying to optimize the geometric configuration in which they exist, e.g., from I_1-over-I_2 to I_2-over-I_1, as shown in **Figure 6**, there is:

a) A topological state in which I_1 is over I_2,

b) A *physically unrealizable* state in which I_1 and I_2 collide –occupying the same 3D space,

c) A topological state in which I_2 is over I_1.

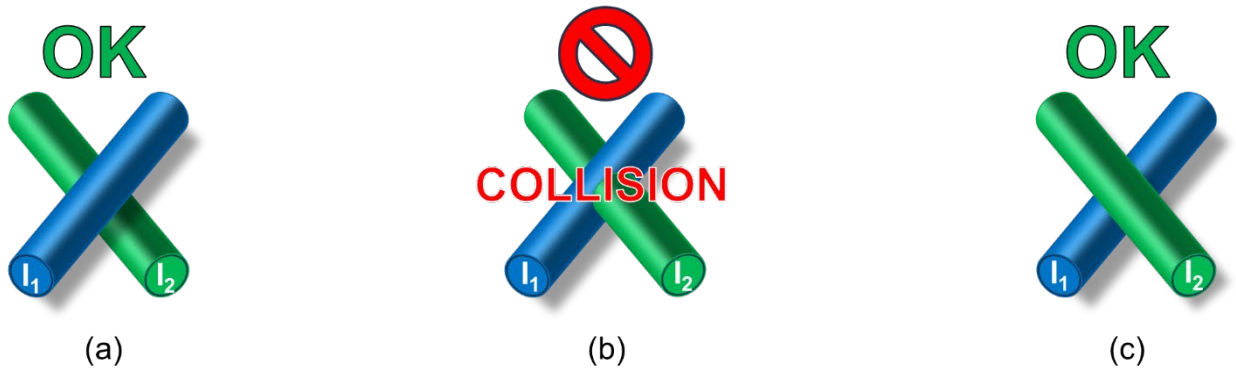

Figure 6: The transition through 3 topological states: a) interconnect I_1 is over interconnect I_2, b) interconnects I_1 and I_2 share 3D volume, which is not a physically realizable state, and c) interconnect I_2 is over interconnect I_1.

The key advantage of optimizing each topological configuration separately, to find its optimal geometric configuration, is that fast, conventional gradient-based geometric solvers would leverage hardware parallelism, and each be kept out of state (b), which is where the gradients typically are challenged due to discontinuous differences in the physics of intervals (a) and (c).

3.2 Assumptions

3.2.1 MDOP Computational Workflow

The proposed computational workflow to solve an MDOP problem is illustrated in **Figure 7**:

- Topological Partitioning transforms the MDOP problem from the infinite, continuous geometric-configuration design space (i), to the infinite, discrete topological design space, shown in **Figure 7 ii**.
- Next, TP identifies Unique Spatial Topologies (USTs) that are simple, by efficient computations that eliminate most of the topological design space by segmenting it into "complexity cones": a simple topology, and an infinite "cone" of undesirably more complex

topologies, as shown in **Figure 7 ii**. A key advantage of TP is the opportunity to simply keep just the simple USTs and eliminate the rest of each infinitely large complexity cone.

  - If one were to consider this problem in the geometric-configuration space, there would be no easy way to collect all the 3D geometric realizations that correspond to the simple UST, let alone those of all the more-complex USTs in its complexity cone. TP provides a convenient handle, UST, and a convenient way to eliminate large undesirable sections of the design space.

- The geometric-configuration space can be imagined looking like a closed-cell foam, as shown in **Figure 7 iii**. TP creates a diverse set of optimization multi-start points to overcome local minima in the closed cell of the geometric configuration space corresponding to each UST, shown in **Figure 7 iii**. For each UST and multi-start point (3D geometric realization of the system): co-optimize the system's component sizing and 3D spatial packaging to find configurations with high-value combinations of:
  - relevant multi-physics-driven value metric(s),
  - spatial compactness value metric of the system configuration, so that it fits within the enclosure, while being physically realizable (no 3D collisions; once it's small enough to fit, additional compactness does NOT add additional value),
  - spatial accessibility of the system configuration: for each component and interconnect in the system, the time and cost of their removal/replacement, weighted by how often they need to be removed/replaced, as a function of their reliability and durability. Cost of removal/replacement can be driven by time to perform the operation, the # of other components and interconnects that must be removed just to get access to this component, the fragility of this component, and its propensity to damage other parts while being removed/replaced itself.

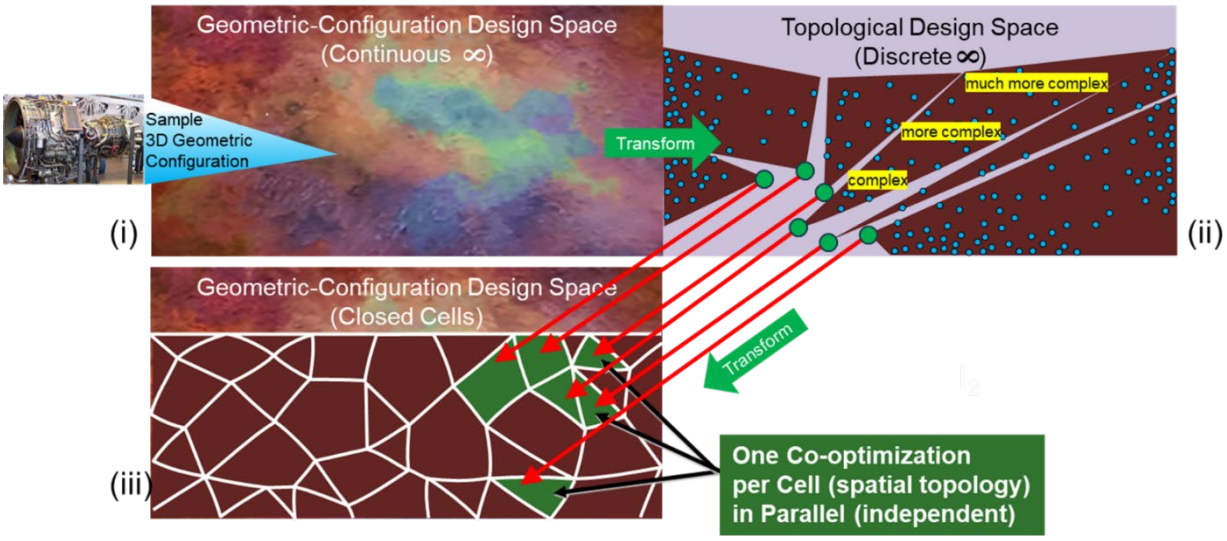

Figure 7: The MDOP Topological Partitioning computational step transforms the MDOP problem from the infinite, continuous geometric-configuration design space (i), to the infinite, discrete topological design space by selecting a very small subset of spatial topologies (green circles in ii) which eliminates infinitely large "complexity cones" of undesirably complex topologies efficiently, and transforms them back to independent contiguous regions of the geometric-configuration space, that are analogous to cells within a closed-cell foam (iii). Each cell that is the target of a selected spatial topology transformed back into this space is the subject of an independent co-optimization of multi-physics-based value-metrics, spatial-compactness value metrics, and spatial accessibility value metrics. The selected cells can be optimized in parallel.

In this closed-cell foam analogy, the cell boundaries are all the 3D geometric configurations that are in state (b) – all the configurations in which one interconnect is virtually crossing thru another, corresponding to configurations that *cannot* be physically realized. The cells, within the closed-cell foam, shown in **Figure 7 iii**, each correspond to a region of configuration space that one optimization solver can focus on to find the global optimum for that cell, meaning the spatially optimum 3D geometric configuration with that cell's topological configuration. So, each cell corresponds to one solver, and the problem is "embarrassingly parallel" (can be parallelized on a core in a cluster/cloud with NO communication required between cores) thus running on N cores provides N x speedup.

3.3 Procedures

3.3.1 Development of Topological Partitioning

The University of Illinois Urbana-Champaign (UIUC) Task 1 Team developed the required Topological Partitioning capability. Technical leadership was provided by Professor Nathan Dunfield, and software architecture and development were provided by Chad Peterson.

3.3.1.1 Tasks

1) Identified candidate approach for topological partitioning – "Complexity Cones":

    1. Identify "cones" (classes of topologies) in topological space, each containing an infinite number of topologies sharing some properties.

    2. Within each cone, at the pointy end of the cone, there are a few simple topologies, while in the rest of the cone, there are increasingly more complex topologies (infinite height of cone), and the more complex they are, the more (combinatoric) versions of each topology there are (area of slice thru cone at any distance from point).

    3. Only the simple topologies in each cone are of interest; the rest of the topologies (the vast majority) are unnecessarily complex, with no added benefit, and considerable added cost, weight, manufacturing challenges, etc.

    4. Enumerating and then rejecting most of the topologies inside each cone is computationally intractable; however, the TP approach algorithmically loops thru the cones, sampling the few simplest topologies from each cone, and simply "ignores" the infinite number of complex topologies in each cone, which are the topologies that are undesirable.

2) Formulated Complexity Cone Mapping Technical Approach:

    1. Begin with one of many possible random 3D layouts of a given system architecture, which describes the components and their interconnections.
    2. Project the system architecture along many different angles in 3D, onto the corresponding 2D planes.
    3. Reject, as complex, any projections with more than a threshold number of interconnect "crossings," in their 2D plane.
    4. For each simple 2D projection, enumerate the combinatorial set of interconnect-crossing sense choices, where either interconnect A crosses over B, or interconnect B crosses over A.
    5. The result is a combinatorial, but finite, set of spatial topologies that includes all simple topologies (the pointy tip of each complexity cone) for the given system architecture, and ignores the entire infinite remainder of each complexity cone.

3) Implemented Yamada Polynomial (YP) Calculator:

    1) Implemented rapid computation of the Yamada Polynomial (topological invariant) for a given topology.

    2) Validated against Yamada Polynomials in [VES1996]. Identified multiple errors in the manual calculations used for preparing that article – verified YP calculator correctness in those cases.

    3) Increased scalability of the Yamada Polynomial Calculator by first reducing the number of crossings in the 2D projection, so that the rest of the Yamada Polynomial computation itself is faster. This enables spatial topologies with many crossings, for which the

Yamada Polynomial computation would be intractable, to first be simplified, and then have their Yamada Polynomials computed rapidly.

4) Task1: Formulated Topological Partitioning Computational Workflow:

   1) Specified the mathematical constructs involved in this workflow and clarified the information they encode, as shown in **Table 1**:

Table 1: Mathematical constructs involved in the Topological-Partitioning computational workflow, and the information that they encode.

Constructs	Components		Interconnects				Notes
	Shape	Location & Orientation	X-sectional Shape	Component Connectivity	Interconnect Trajectory	Spatial Topology	
System Architecture[1]	Y[2]	N[3]	Y[4]	Y	N	N	1. Input to Topological Partitioning Workflow 2. Indirect reference to Component Geometry Model 3. System Architecture doesn't specify Component 3D Locations or Orientations, but may include constraints on Locations (e.g., Compressor in Fuselage, Coaxial with Turbine; HX in Duct A, with primary flow along Duct A, and 2ndary crossflow horizontal) 4. Cross-sectional shape of wires, pipes, ducts.
Spatial Graph (SG) encoded as Spatial Graph Diagram (SGD)	N[5]	Y[6]	N[7]	Y	Y[8]	Y	A SGD includes 2D Relational component and interconnect info, but not *absolute* locations or trajectories. The SGD also includes annotation of the angular order of interconnect entry/exit to/from each component, and the z-order of the interconnects at each crossing. 5. Arbitrarily thick graph nodes (not points) 6. Relational; 2D 7. Arbitrarily thick edges 8. Relational; 2D; crossings: z-order
Yamada Polynomial	N	N	N	N	N	Y[9]	9. YP uniquely identifies SGs, encoded as SGDs, that share the same Spatial Topology
Geometric Realization (GR)	3D	3D	3D	Y	3D	Y[10]	10. GR is a 3D instance of a Spatial Topology

2) Formulated the transformations, between constructs, that are used in this workflow, as shown in **Table 2**:

Table 2: The transformations between constructs used in the TP computational workflow.

To: **From:**	**System Architecture**	**Spatial Graph (SG) encoded as Spatial Graph Diagram (SGD)**	**Yamada Polyno-mial**	**Geometric Realization**
System Architecture		**Module 1**		
Spatial Graph (SG) encoded as Spatial Graph Diagram (SGD)	Extract SGD Connec-tivity Attribute	Reidemeister Moves	**Module 2**	**Module 3**
Yamada Polynomial				
Geometric Realization (GR)	Extract GR Connec-tivity Attribute	**Module 4**		**Module 5**

- **Module 1:** Enumerates all Spatial Graph Diagrams from simple to complex, up to a given number of interconnect crossings.
- **Module 2:** Computes Yamada Polynomial of a Spatial Graph Diagram. All SGDs that share the same Spatial Topology have the same YP.
- **Module 3:** Generates a 2D planar realization of the Spatial Graph, and then, at each 2D interconnect crossing, displaces the two interconnects out of plane, creating a 3D near-planar geometric realization.
- **Module 4:** Projects the 3D Geometric Realization onto a 2D plane so that all inter-connect crossings involve only 2 interconnects, and then annotates components with angular order with which interconnects enter/exit, and annotates crossings with the z-order of their 2 interconnects (over/under).
- **Module 5:** Takes a near-planar 3D Geometric Realization and applies stochastic force-directed layout, and 3D rotation, to generate a set of GRs. Applies a physically relevant diversity metric to select a given number of maximally diverse GRs as start points for geometric optimization, to overcome the obstacle of many local minima.

3) Formulated the Topological Partitioning Workflow, comprised of these transformations as shown in **Figure 8**:

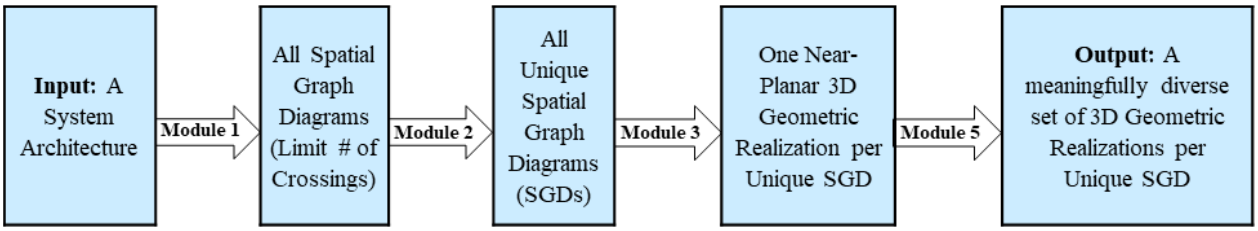

Figure 8: The transformations that constitute the modules of the TP computational workflow. Note that Module 4 is used to verify that all Output GRs generated by Module 3 and Module 5 preserve the Spatial Topology of the unique SGD from which they were generated.

5) Generated Meaningfully Diverse 3D Geometric Layouts: Formulated a quantitative metric for assessing meaningful diversity of 3D geometric layouts of a spatial topology, and an efficient approach to generate meaningfully diverse 3D Geometric Realizations (3DGRs) efficiently.

   Topological Partitioning is done, within MDOP, to enable Geometric Optimization to proceed separately, within each cell in the geometric design space, corresponding to one spatial topology. Within each cell, there are often many local minima, since MDOP is typically most useful for 3D packaging problems with high packing densities – so each component or interconnect can be moved slightly before colliding with another component or interconnect.

   To overcome the optimization obstacle of many local minima, a standard optimization approach is to identify a diverse set of starting points, from which to begin the optimization. In this case, MDOP is producing a diverse set of 3D Geometric Realizations, corresponding to each Spatial Topology, as starting points for geometric optimization within the corresponding cell.

   Module 5 applies stochastic force-directed layout (FDL), which is non-deterministic, so each time FDL is run, a somewhat different resulting 3D Geometric Realization is generated as shown in **Figure 9**. In addition, a random 3D rotation orients the GR differently with respect to (w.r.t.) the packaging volume and its external interfaces. **Module 5** then applies a physically relevant diversity metric to select a given number of maximally diverse GRs as start points for geometric optimization.

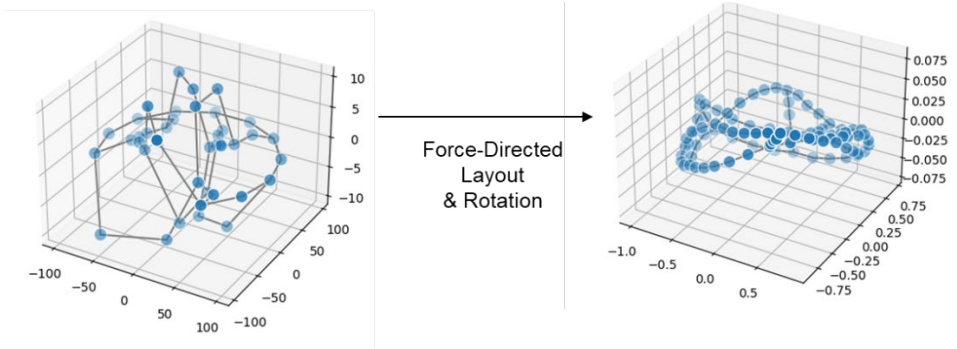

Figure 9: Stochastic force-directed layout, with 3D rotation, to generate a set of 3D Geometric Realizations from which a diverse set can be selected.

Module 5 generates a given number of GRs for each near-planar GR. Next, it combines sets of GRs from different near-planar geometric realizations originating from the same unique Spatial Graph Diagram. For each GR corresponding to the same unique SGD, Module 5 identifies the N closest components or interconnect elbows (waypoints inserted along interconnects to enable piece-wise linear "curved" interconnects) to each of several important static external sources of thermal, acoustic, electromagnetic interference (EMI), or other physical fields, or external components or interconnects that are sensitive to physical fields generated by the system being packaged. The large set of GRs is then clustered (K-means clustering) into sets of GRs having similar physically relevant adjacencies, as shown in **Figure 10**, and the most compact GR in each cluster is selected. These are the starting points for the geometric optimization of the associated unique SGD and its Spatial Topology. An example is shown in **Figure 11**.

The purpose of making the 3D geometric realizations (start points) meaningfully diverse, is to leverage what we understand about the physics of the problem to aim for 1 start point per basin of attraction, where the basins of attraction are based on the interaction of the physics and the spatial topology.

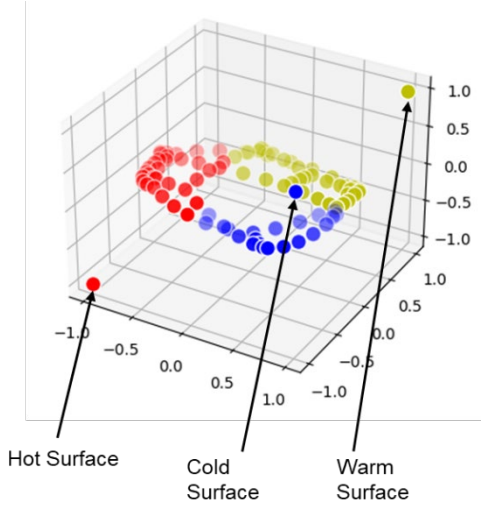

Figure 10: A physics-based diversity metric that considers, for each 3D Geometric Realization, which components and elbows are closest to a set of physically relevant external locations.

Module 4 was used to test that the resulting diverse set of GRs generated from each unique SGD have the same Yamada Polynomial, indicating that they do indeed share the same Spatial Topology. This testing was successful, indicating that **Module 3** and **Module 5** preserve Spatial Topology.

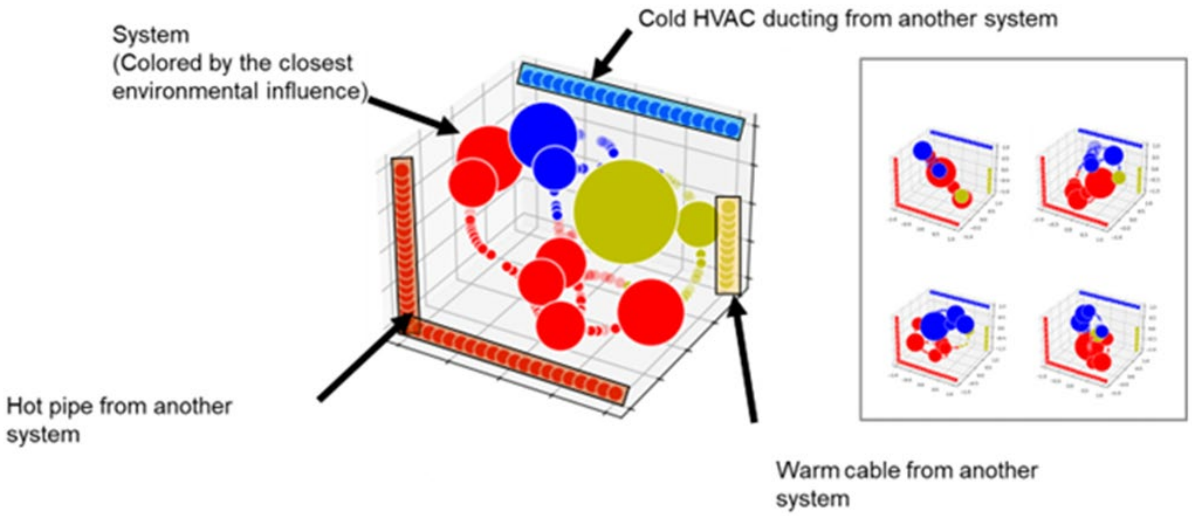

Figure 11: Example: in one geometric realization, a heat-sensitive component is adjacent to a hot pipe of another system. In another geometric realization, it is near the cold heating, ventilation and air conditioning (HVAC) ducting.

6) Assessed the scalability of the Topological Partitioning workflow steps and identified 2 primary paths for improving scalability (**see section 4.1.1 item 10**).

3.3.2 Development of Co-Optimized Physics and Spatial Configuration

The University of Connecticut (UConn) Task 2 Team developed the necessary Co-Optimization, Physics, and spatial Configuration capability. Technical leadership was provided by Professor Horea Ilies, algorithmic development and software development was provided by Mohammad Behzadi, and software architecture for graphics processing unit (GPU) pipelining was provided by Peter Zaffetti.

3.3.2.1 Tasks

1) Developed and demonstrated initial 2D and 3D spatial optimization of a set of a few interconnected components, represented using MDBD, as a baseline capability, as shown in **Figure 12**:

- 2D:

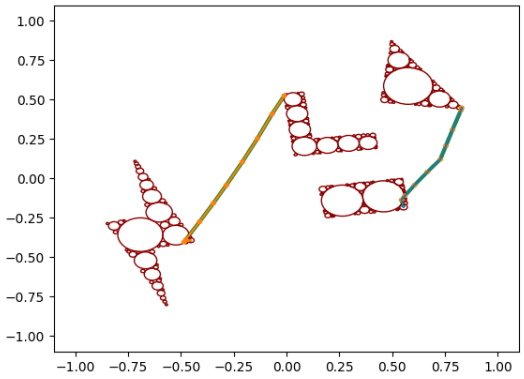

- 3D:

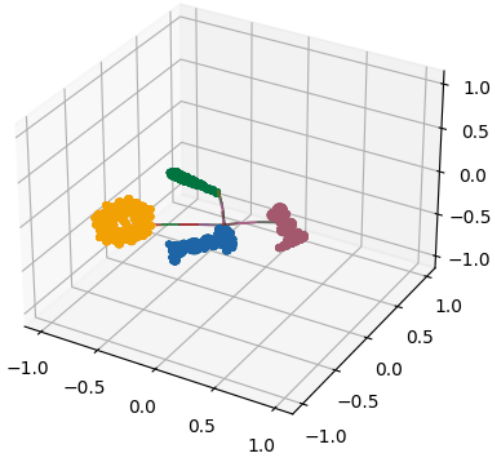

Figure 12: 2D and 3D spatial optimization using MDBD.

2) Demonstrated MDBD's support for dimension elevation, from a 3D packaging problem, up to four-dimensional (4D) to avoid a local minimum, and then back down to a 3D result, as shown in **Figure 13**.

   MDBD enables the geometric problem to be elevated from its native dimension, when the optimization encounters a local minimum, up one or more dimensions, so that the optimization can continue, without collisions in this higher dimension, and then project back down to the problem's native dimension, to continue optimization.

   As shown in **Figure 13**: An illustration of the concept of using dimensional elevation, in geometric optimization, to avoid local minima, a simple 2D → 3D → 2D illustration of dimension elevation to optimize past obstacles (local minima) is:

   1. a 2D disc inside a square frame (**Figure 13a**).
   2. The disc is optimized in the direction of the objective function and reaches a local optimum in the top-right corner. (**Figure 13a**).

3. Dimension elevation to 3D enables translation below the frame (**Figure 13b**).
4. Optimization in 3D proceeds until the disc is past the frame (**Figure 13b**)
5. Projection back to 2D.
6. Enables optimization to continue in 3D (**Figure 13b**).

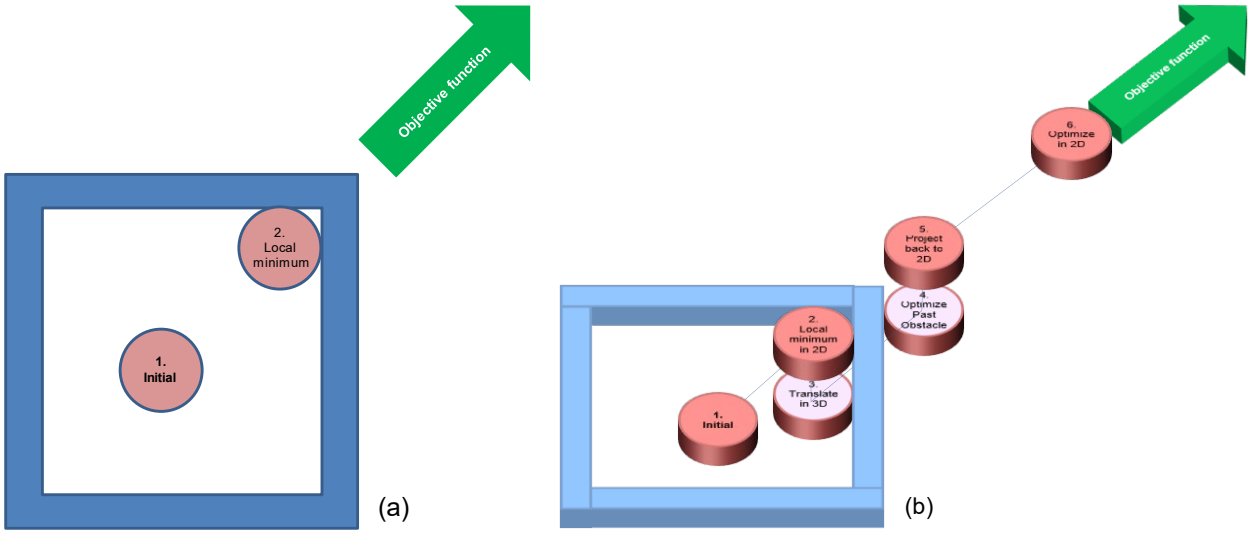

Figure 13: An illustration of the concept of using dimensional elevation, in geometric optimization, to avoid local minima.

3) As shown in **Figure 14**, a simple example was implemented using MDBD with a toroidal component and an interconnect between two cube-shaped components:

- The initial condition, with the interconnect outside the torus (**Figure 14a**). The geometric optimization attempts to shorten the interconnect and decrease the bounded volume.
- Without dimension elevation, in 3D, the optimization reaches a local minimum, and the interconnect gets stuck, unable to pass thru the torus, as the interconnect's length is minimized (**Figure 14b**).
- With dimension elevation, from 3D to 4D, the optimization proceeds in 4D, past the torus, until it can pass thru the hole in the torus. After projection back from 4D to 3D, the optimization proceeds onward, shortening the interconnect so that it passes thru the center of the torus (**Figure 14c**).

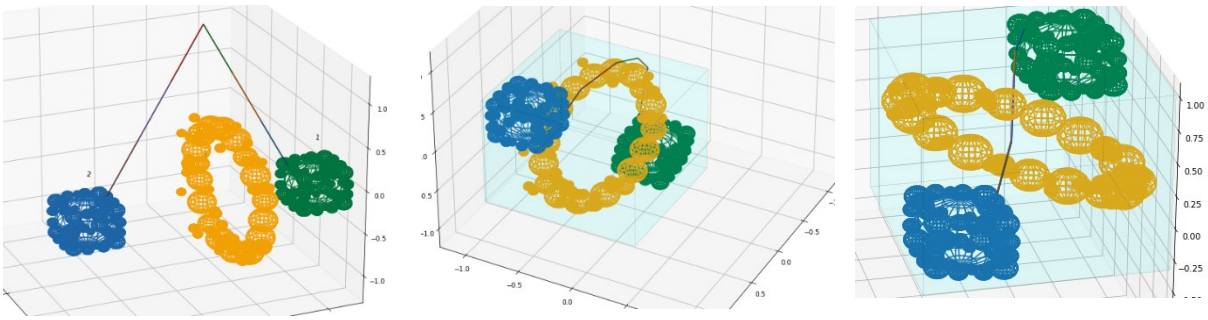

Figure 14: An example of geometric optimization, using MDBD with dimensional elevation, to avoid local minima. (a) initial condition, (b) w/o dimension elevation, the optimization reaches a local minimum with the interconnect stuck on the torus, and (c) with dimension elevation: interconnect proceeds past torus for compact packaging.

4) A more complex example was implemented using MDBD with a set of 6 interconnected cube-shaped components (**Figure 15**):

   - The initial condition, with the interconnect blue and orange components far from one another (**Figure 15a**). The geometric optimization attempts to shorten the interconnects and decrease the bounded volume.
   - Without dimension elevation, in 3D, the optimization reaches a local minimum, and the orange component gets stuck, unable to pass thru the yellow component, as the bounding volume is minimized (**Figure 15b**).
   - With dimension elevation, from 3D to 4D, the optimization proceeds in 4D, with the orange component moving past the yellow component, until the blue/orange interconnect can be reduced in length again. After projection back from 4D to 3D, the optimization proceeds onward, shortening the interconnects and moving the components so that they are all in a plane, and as close to one another as allowed by the problem constraints (**Figure 15c**).

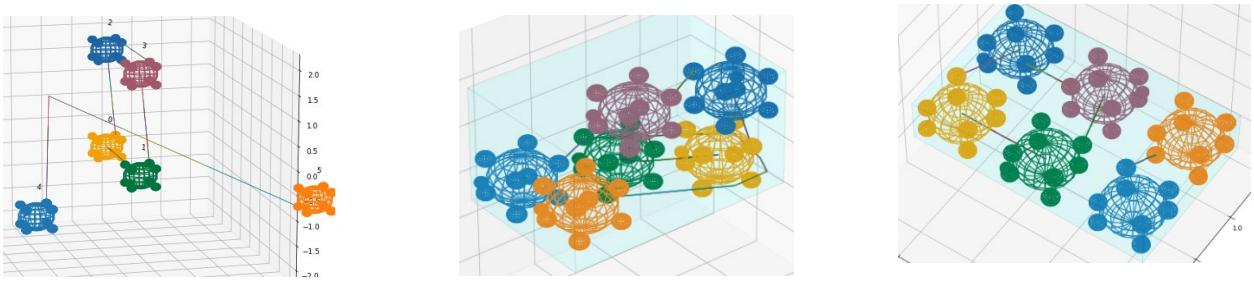

(a) (b) (c)

Figure 15: An example of geometric optimization, using MDBD with dimensional elevation, to avoid local minima. (a) initial condition, (b) w/o dimension elevation, the optimization reaches a local minimum with the interconnect between the blue (top right) component and the orange component stuck on the yellow component (e.g., the orange component cannot go farther down to the right to get around the yellow component because that would increase the packaging volume), and (c) with dimension elevation: orange component proceeds past yellow component for compact packaging near bottom blue component.

3.3.3 Development of Spatial Accessibility Value Metrics

The UIUC Task 3 Team developed the required accessibility value metrics. Technical leadership was provided by Professor Nancy Amato, algorithm development was provided by Stav Ashur, and Isaac Love.

3.3.3.1 Tasks

1) Identified a preliminary list of relevant measurable accessibility attributes of a 3D geometric realization that drive life-cycle cost, and that are candidate elements of a process-cost predictive metric formulated for a set of required removal/replacement operations (a spatial value metric) within a design optimization objective function:
    - The spatially driven life-cycle cost can be expressed as:

      (removal & replacement cost) x (removal & replacement frequency)

    - Removal & replacement cost can be decomposed into:
        - Costs associated with each component and rigid interconnect. These removal & replacement costs are a function of:
            - **Path length**: trajectory of component center-of-mass (expressed path as piecewise linear waypoints of component/interconnect center-of-mass, and orientation).
            - **Path width**:
                - Area (cross-sectional).
                - Minimum width: pinch point (cross-sectional: fixed or ideal component rotation angle around path centerline).
                - Average width along path.

        - Minimum clearance (assuming fixed or ideal component rotation angle).
        - Sensitivity of component clearance to component rotation out of cross-sectional plane.
        - Risk-weighted (by likelihood of accidental contact & fragility of parts along path that may be damaged by accidental contact with component due to proximity).
    - **Path tortuosity:**
        - Zig-zag pattern: L/R/L/R...
            - Angles of course changes along path.
            - Total number of course-changes along path.
        - Line of sight along path: *f* (path width & tortuosity).
        - Corkscrew/spiraling.
        - Total change in orientation of part required along path.
    - **Tooling accommodation**
        - Room to plug/unplug, connect/disconnect component.
        - Elbow room, wrist room to remove/replace component.
        - Wrench-swing/tool-operation.
            - Confined space dimensions.
            - Required torque and time to operate tool with limited range of motion.
- Alignment of required tool-force direction with axis of path leading to that location.
- Costs associated with each **flexible interconnect**: these include the same costs listed above for rigid interconnect plus additional costs associated with "floppiness" of flexible wires, cables, hoses, and wire harnesses. These extra costs are a function of:
    - Number of support points required to carry interconnect.
    - Number of joints that can be flexed to re-orient interconnect: this refers to the ability to pre-fold or configure a flexible interconnect into a compact shape.
    - Range of flex angle at each interconnect joint (a flexible interconnect can be considered as a discretized set of piecewise linear lengths with joints between them, or as an integral strand that can be looped).
    - Range of twist angle at each interconnect joint.
- Costs associated with necessary removal and replacement of other components and/or interconnects that prevent the subject component or interconnect from being removed and replaced. Since components/interconnects can **block** one another, there is a hierarchy of components/interconnects to remove and replace. So, for each component/interconnect in the system architecture, given the 3D Geometric Realization, each component/interconnect requires all components/interconnects below it in the tree, to be removed first and replaced afterwards.

2) Prototyped assessment of 3 of those attributes on alternative spatial packaging configurations:

- Path Length.
- Path Width (**Figure 16**): Risk weighted by proximity & fragility (**Figure 17**).
- Path Tortuosity: Total number of course-changes along path.

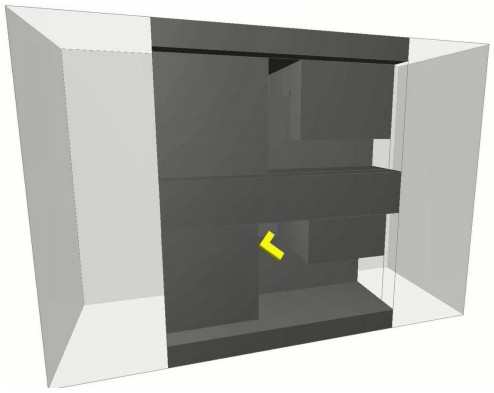

Figure 16: Snapshot of simulation video showing lower path selected due to path width.

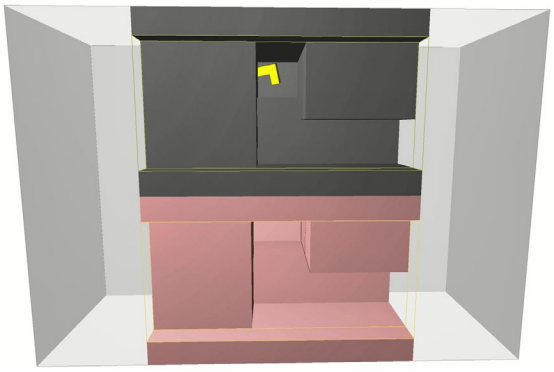

Figure 17: Snapshot of simulation video showing upper path selected due to risk-weighted cost (proximity and fragility) of lower wider path exceeding the cost of the narrower upper path.

3) Prototyped identification of the hierarchy of components that indicates which subset of components are **blocking** the component of interest, and therefore must be removed to enable each other component to be removed (Replacement sequence is reversed). That hierarchy is used to compute the third major element of removal and replacement cost, as shown in **Figure 18**.

	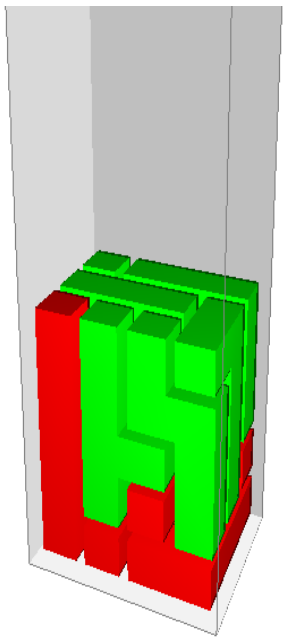	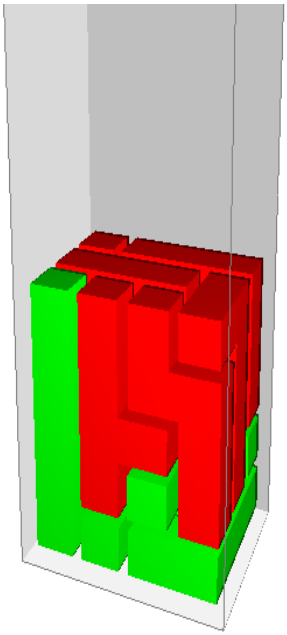
Open access to packaging volume	top	top
Components needing **frequent** service:	top	Bottom
Components needing **infrequent** service:	bottom	top
Total cost:	389 (better)	524 (worse)

Figure 18: Two examples of "blocking," as an element of removal and replacement cost. Note than when the components needing frequent service, and thus frequent removal/replacement were on the top (easiest access), the cost was better, and when they were buried on the bottom, they were blocked by many other components, so the cost was worse.

4) Demonstrated Preliminary Results for Task 3 (Presented by UIUC 7/21/2023)

- Can compute accessibility metrics for a component (computationally costly):
  - Distance
  - Clearance (minimum, average)
  - Weighted clearance w.r.t. component properties
- Can compute a Life Cycle Cost score of an assembly based on components' removal paths and frequencies of removal/replacement.

3.3.4 Development of Co-Optimized Physics, Spatial Configuration and Accessibility

The UConn Task 2 Team also developed the Task 3 Co-Optimization and Accessibility capability.

3.3.4.1 Tasks

1) Formulated Co-Optimization Approach Including Accessibility:

Considered a variety of technical approaches that address 3 fundamental computational tasks. For this topic, a component or interconnect is simply referred to as an "object":

1. Identify object removal/replacement paths.
    - Sampling-Based Motion Planning (SBMP) (T. McMahon, 2014) (demonstrated for computing preliminary accessibility metrics in Task3 preliminary work).
    - Convolutional methods (fast fourier transform (FFT)-based).
    - Pattern flood-fill based methods (projection).
    - Raytracing based methods (GPU).
2. Identify blocking list/tree, of all objects that must be removed/replaced to enable a given object to be removed/replaced. This enables an object's own cost of removal/replacement to be compounded by the cost of all other objects required to be removed/replaced to gain access to it.
    - Path planning with collision detection.
    - Simplified common-axis removal paths with collision detection.
    - Simplified common-axis removal paths with ray tracing methods.
3. Evaluate accessibility metric based on removal/replacement paths of each given component or interconnect, and the removal/replacement cost of each component and interconnect in the blocking tree that blocks the given component or interconnect.
    - Path length:
        - compute geometrically from path.
        - use ray tracing light intensity as surrogate for path length.
    - Path clearance:
        - compute geometrically from path and other objects.
        - use ray tracing light distribution (or angle of it at each point) across safe zone as surrogate for path clearance.
    - Risk-weighted path clearance:
        - compute geometrically from path and other objects.
        - assign rough texture to fragile or dangerous objects, so they reflect light off-axis, and then measure light distribution (or angle of it at each point) across safe zone as surrogate for risk-weighted path clearance.

2) Inclusion of Coarse Accessibility Value Metric into Co-Optimization:

- **Defined "accessibility importance" input parameter:** This input parameter indicates the importance of accessibility for an associated component. If a component has short life and/or low reliability, then it must be inspected, removed and/or replaced often, so it is important that it be easily accessible (i.e., should require removal/replacement of as few other components as possible). On the other hand, a component with long life and/or high reliability requires inspection, removal and/or replacement rarely, so it is not important for it to be easily accessible, especially at the expense of other components with higher accessibility importance.

- **Defined "accessibility window" of enclosure**: The "accessibility window" is one wall of the enclosure, through which components will be accessed. For an automotive engine compartment, the accessibility for a novice mechanic would be the top surface (where the hood goes when it's closed), and for an advanced mechanic we'd define both top and bottom accessibility windows. Initially, we'll assume that there's only one accessibility window. We'll also simplify the problem by assuming that components are removed only perpendicular to the accessibility window, e.g., up out of the car's engine compartment.
- **Defined, developed, and tested a coarse accessibility value metric algorithm:** The task 3 team defined an algorithm to compute a coarse accessibility value metric. The algorithm computes the number of other components along its path toward the accessibility window – those are the components that are blocking it – i.e., they must be removed before the subject component can be accessed. The component's accessibility importance parameter is multiplied by the number of blocking components, and this product is summed across all the components. The lower the sum-product, the more accessible the system configuration is. In addition, a set of tool-operation (e.g., wrench-swing) 3D volumes were defined – one per component – representing the operation of tooling (a wrench, screwdriver, gripper, etc. used to disconnect/reconnect the component during removal/replacement, or to diagnose the trouble during repair). These tool-operation volumes are each associated with a component and must be made accessible before the component can be removed/replaced. However, since these volumes are air (empty), they can't block another component, and can occupy the same 3D space as other components that must be removed before this component is accessible. The component's number of blocking components is the number of unique components that block either it or its tool-operation volume. This algorithm was tested and demonstrated in the co-optimization, as shown in **Figure 19**.

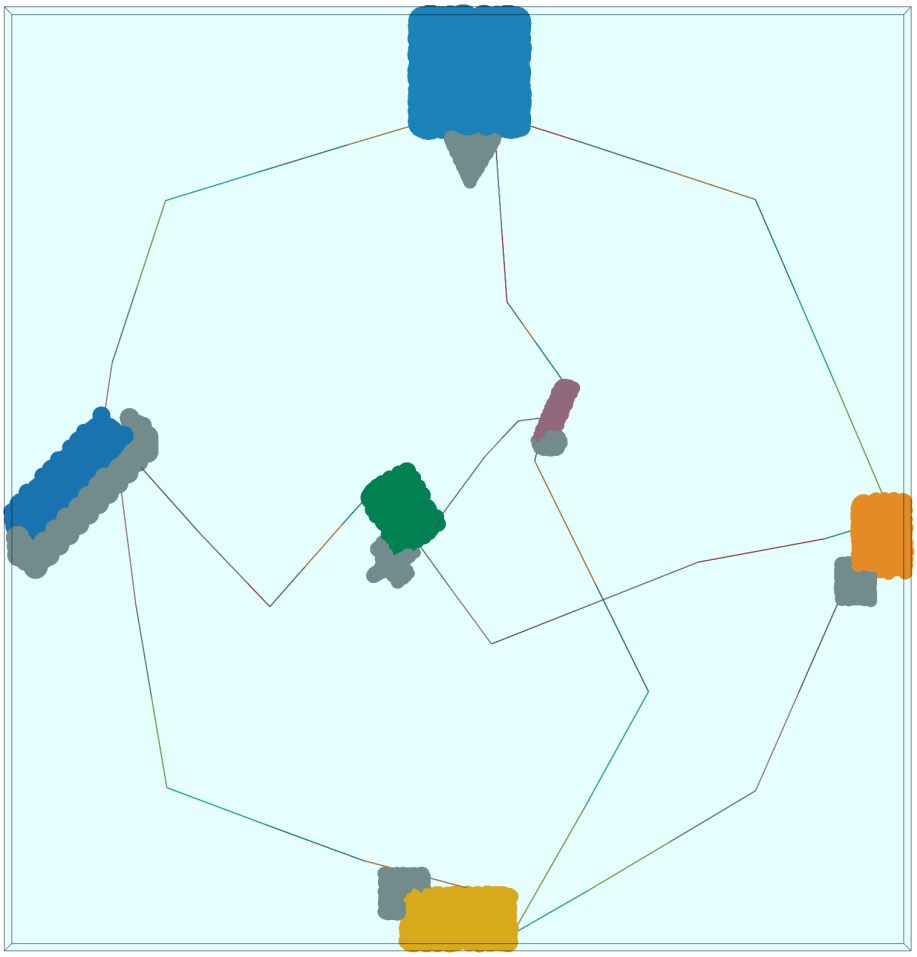

Figure 19: A Graphics Interchange Format (GIF) showing co-optimization of spatial compactness and spatial accessibility.

3) Profiled the co-optimization workflow, shown in **Figure 20**.

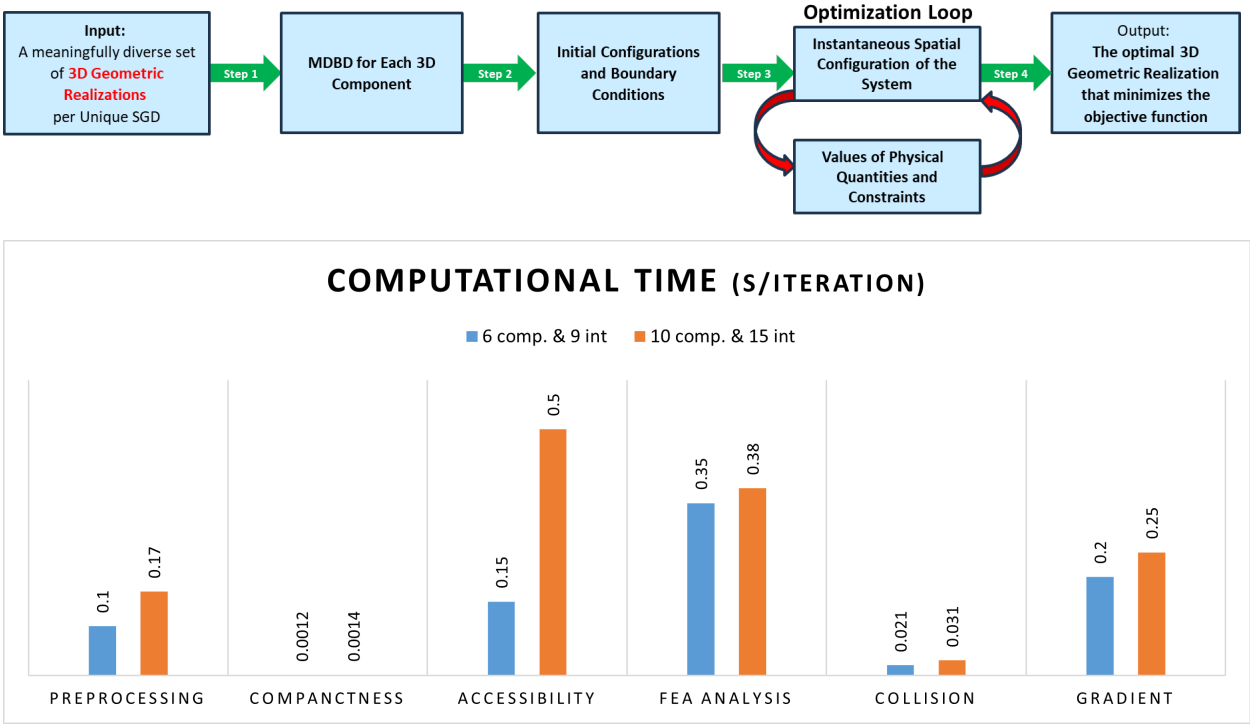

Figure 20: Computational profiling results of the co-optimization workflow shows spatial accessibility scaling poorly, and the gradient (which is being replaced in Task4).

4) Focused on the accessibility and gradient calculations as primary sources of scalability limitations. Did *not* focus on finite element analysis (FEA), since the physics is application specific (not MDOP specific). Estimated that 10x-100x scalability improvement can be achieved by removing GPU-to-central processing unit (CPU) synchronizations, which requires additional assumptions to remove CPU-side logic for sensing convergence.

5) Gathered data quantifying how the relative value metrics compete during co-optimization, and used these observations to propose and implement two improvements to the co-optimization:

   - Found that combining translation and rotation at each optimization step, converged to the best solutions vs. alternating periods of optimizing translation and rotation separately.
   - Found that occasionally separating the components in all directions, converges to the best solutions vs. simply optimizing without the occasional separation, because separation enables components more freedom to get past one another.

6) Measured the computational time for accessibility computations during co-optimization (**see 4.1.2**):

   - 10 components, 100 spheres = 0.5 sec/iteration

- 100 components, 100 spheres = 50 sec/iteration

7) Estimated that 10x to 100x speedup can be obtained, in computing the accessibility value metric, by combining matrix operations. Spatial hashing (Dong, 2021) is also a possibility.

8) Reframed the accessibility computation, for speedup, by limiting the consideration of blocking components to only those within range to block the subject component geometrically.

3.3.5 Validation

The Raytheon Technologies Research Center (RTRC) Task 4 Team performed validation. Technical leadership, challenge problem distillation, and optimization architecting was provided by Joe Turney, algorithm development and data-structure design was provided by Raphael Mandel, and challenge problem elicitation was performed by Shane Haydt.

3.3.5.1 Tasks

1) Integrated the National Aeronautics and Space Administration's (NASA) Open Multi-Disciplinary Analysis & Optimization (OpenMDAO) framework in an object-oriented (modular) fashion, as shown in **Figure 21**, so that the physics code would be included as a module that could be replaced by any other drop-in physics replacement module when Raytheon Technologies Corporation's (RTX) background intellectual property (IP) was removed.

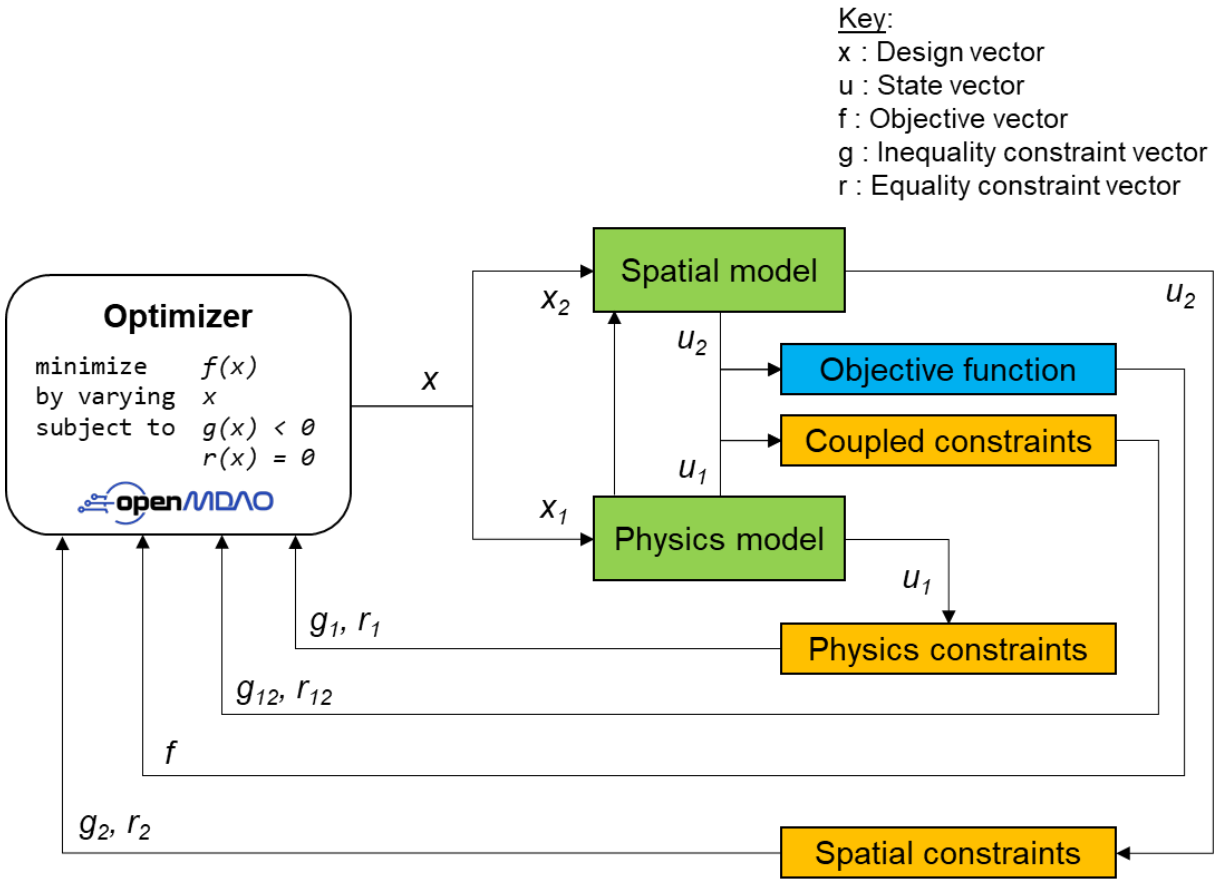

Figure 21: An RTX physics-sizing model has been integrated to the spatial model in a modular fashion within OpenMDAO. The optimization problem has been fully flattened so that the OpenMDAO optimizer provides a design vector to each model (physics, spatial). The physics and spatial models are called independently; coupling is done entirely via constraints, other than the physics model passing the updated component and interconnect geometry to the spatial model for configuration.

2) For the **Spiral2 challenge problem**, there is a complex-geometry enclosure, a duct, within which the heat exchanger(s) must fit as they are resized, reshaped, relocated, and re-oriented during co-optimization iterations. The university subcontractors did not distinguish the separate notions of a spatial-compactness value metric and a specified, complex 3D geometric enclosure, within which the relevant components and interconnects must always remain throughout the co-optimization, without colliding with one another.

   The university subcontractors' spatial-compactness metrics were a bounding volume that could be computed based on the components, and a total interconnect length.

   The Task4 Validation team identified that better understanding was needed regarding how the spatial constraint needs to be expressed as the geometry of the enclosure is considered. The **Spiral1 challenge problem**, created to provide and test that understanding, consists of a heat exchanger (HX) in a box, optimized to improve physics-based value metrics: higher effectiveness and lower pressure drop (larger size). The HX must rotate into alignment with a diagonal plane of the box to enable growth and must always remain inside the box.

The **Spiral1.5 challenge problem** was created to provide and test similar understanding regarding interconnect optimization. It consists of a single interconnect with straight segments connecting multiple elbows (way points). The interconnect is optimized to reduce a physics-based value metric: lower pressure drop, which is composed of line losses and turning losses. The interconnect must align to form an s-shaped curve, by moving the elbows accordingly.

Once the Spiral1 and Spiral1.5 challenge problems yielded the necessary understanding and working implementations of spatial constraints for components and interconnects, the Task4 Validation team approached the Spiral 2 challenge problem.

3) Defined the data structure for and geometry of the inlet and outlet interconnects and the HX and implemented software to generate physics-based sensitivities for MDAO to improve HX effectiveness and decrease pressure drop, leveraging physics-based models that are RTX background IP.

   As shown in **Figure 22**, each interconnect, between an origin component and a destination component, consists of N straight segments and N+1 turns, connecting an output port on the origin component to an input port on the destination component. Straight segments are represented by a line of overlapping spheres, with the number of spheres inversely related to the interconnect diameter (and thus their diameter). Diameter is constant along each interconnect. This spherical representation is extensible to more complex duct shapes. Fluid interconnects cause loss in potential:

   - Pressure loss = f(D, L, θ, w, ρ, μ)
   - Voltage drop = f(D, L, I, σ)

4) Specified the interconnect spatial model and its data structure, as shown in **Figure 22**.

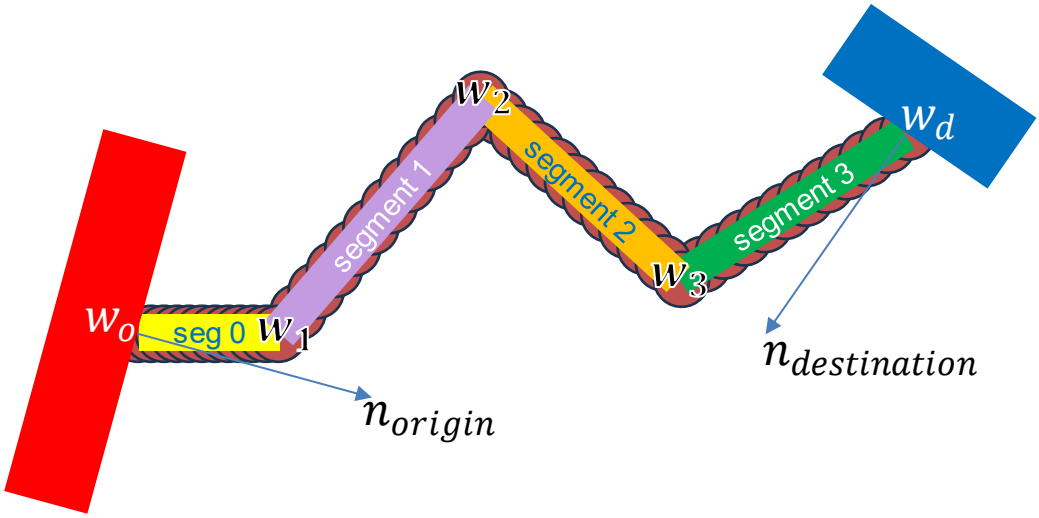

Figure 22: Specification of interconnect spatial model: N straight segments, connecting N+1 waypoints, with each segment populated with overlap-ping spheres.

5) Applied the lessons learned and spatial constraint-modeling approach from Spiral1 to specify the enclosure Keep-In and Keep-Out zones for Spiral 2.

The Task4 Validation team determined that both a Keep-In zone and a Keep-Out zone were required to manage keeping the HX, inlet and outlet inside the enclosure. It was difficult to ensure that a component was entirely within the Keep-In zone.

6) Validation Spiral 3:

   - The Task 4 team defined the Spiral 3 challenge problem required to validate the Task1-3 MDOP workflow elements to optimally pack and route the components and interconnects within an RTX proprietary UAV design, including the propulsion system, and the power and thermal management system. It also includes payload, etc. as obstacles, within the UAV body's inner surface, which serves as the enclosure.

4.0 RESULTS AND DISCUSSION

4.1 MDOP Computational Workflow Demonstrated at Small Scale

4.1.1 Topological Partitioning Demonstrated

1) Implemented and tested the Topological Partitioning Workflow, including generating multiple meaningfully diverse 3D geometric layouts, shown in **Figure 23**, per spatial topology:
2) Associated 3D component geometry with system architecture
   - Applied the TP computational workflow to a simple example with 6 nodes, 9 edges and 1 crossing.
   - The diversity metric considers physical proximity between components and interconnects of the system and both:
     - physical field sources external to the system (e.g., hot objects within the packaging volume that can radiate heat to portions of the system, affecting its SWAP-C metrics), and
     - physical field sources internal to the system (e.g., hot components or pipes/ducts that can radiate heat to other thermally sensitive components or interconnects, affecting the system's SWAP-C metrics).

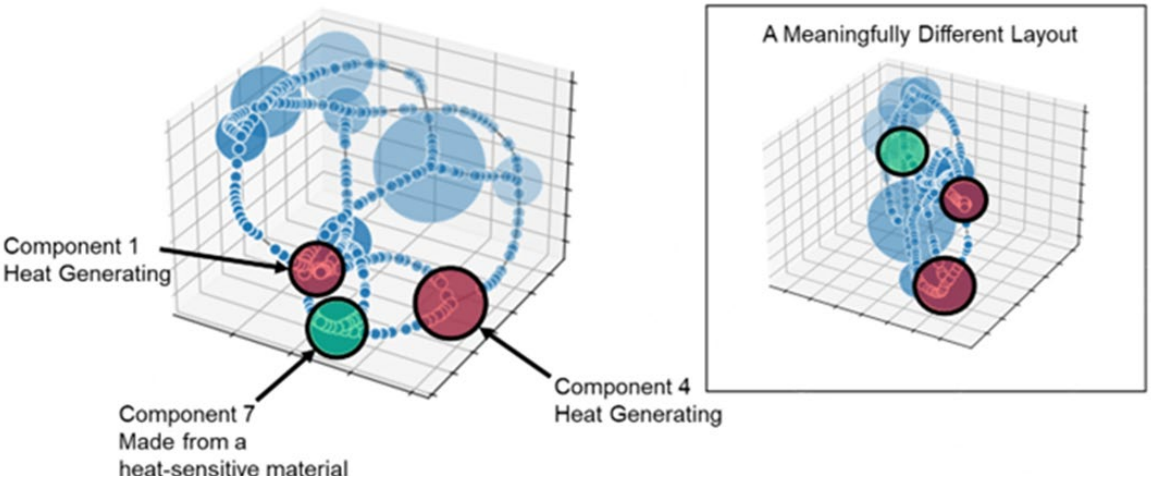

Figure 23: In the left geometric realization, the heat-sensitive component is sandwiched between two hot components. In the right geometric realization, it is far away from both.

   - Module 5, in the TP Computational Workflow, generates many 3D geometric realizations for each unique Spatial Graph Diagram (<1 sec each), and uses this new physically meaningful diversity metric to select the 3D geometric realizations to use as start points for the Geometric Optimization, as shown in **Figure 24**:

3) Applied the TP computational workflow to a more complex example with 10 nodes, 13 edges and 4 crossings, as shown in **Figure 25**.

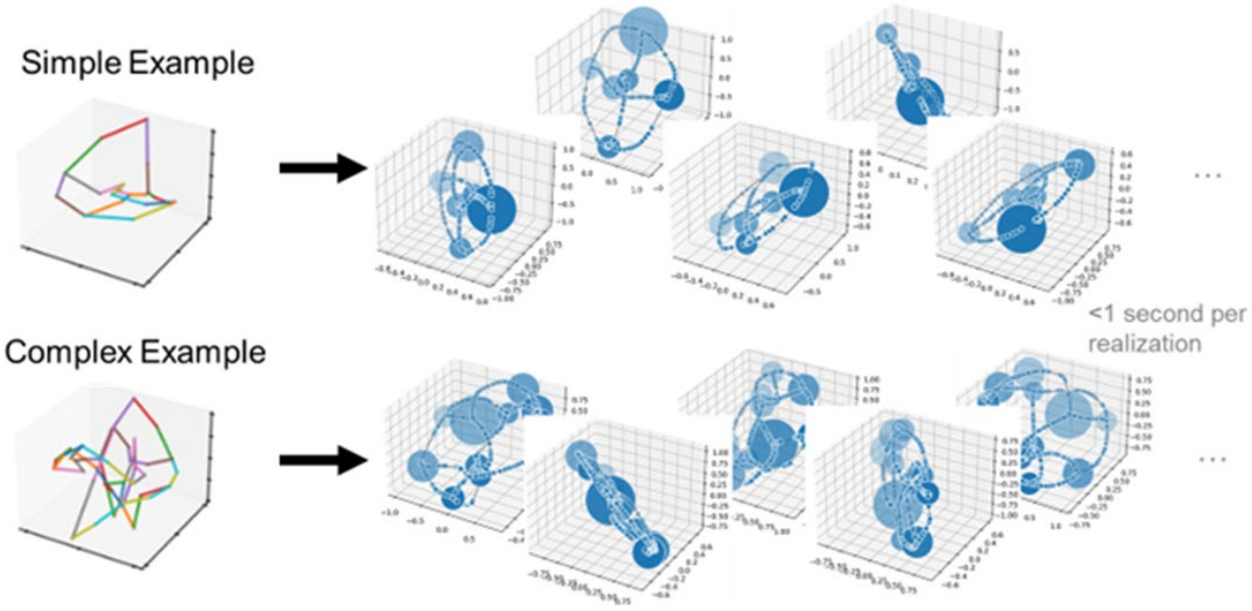

Figure 24: Module 5 Examples. NOTE: This process is NOT random -- it preserves the Unique Spatial Topology.

- Determined that Modules 1 & 2 are exponential, with Module 1 becoming intractable after roughly 14 components and 14 interconnects.

4) Identified 2 primary paths for improved **scalability**:

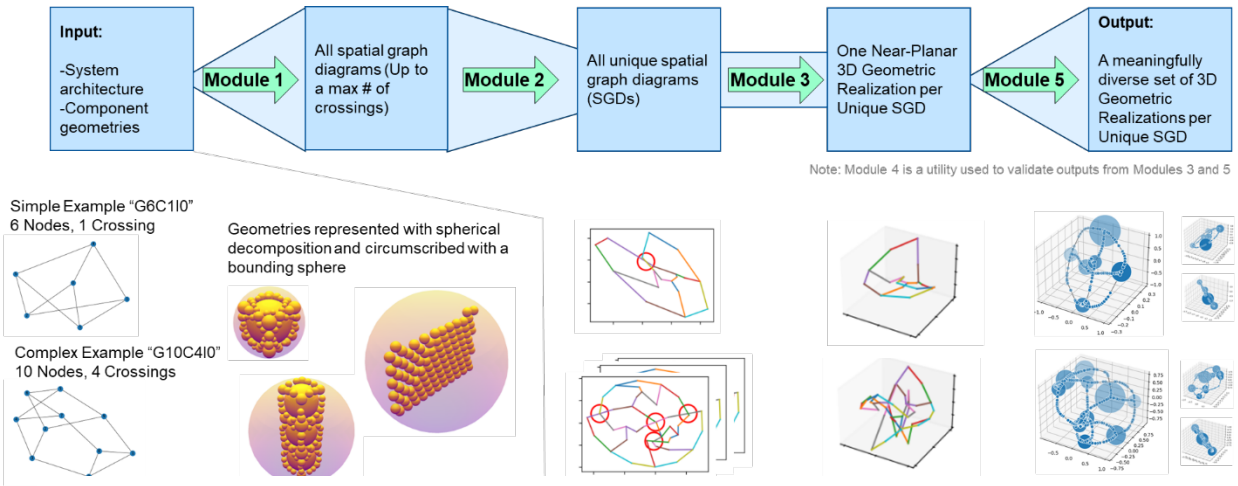

Figure 25: The Topological Partitioning (TP) computational workflow applied to 2 examples.

- **Path 1: Sampling SGDs with Diversity**: At 20 or 30 components, and 20 or 30 interconnects, the number of crossings goes up substantially, even among the spatial graph di-

agrams in the simple ends of the complexity cones, so that individual pairs of interconnects have very few crossings, and yet the total number of relatively simple SGDs grows combinatorically, so that enumerating them is intractable.

- There are many sampling strategies with which to select a manageable number of SGDs from all those that exist.
- Due to the enormous design space of SGDs in this case, the probability of any two corresponding to the same Unique Spatial Topology is extremely low, so that Module 2's function changes from finding unique SGDs to a more useful function in this case: it becomes more useful to make random crossing changes to each sampled SGD, until it matches another one of the sampled SGDs. This will provide a quantitative metric for diversity of the sampling strategy.
- It would be productive to compare sampling strategies to determine which provide the best topological diversity.

- **Path 2: Sequential Packing, then Routing with Diversity:**
  - Recent improvements in rapid bin-packing computations (Qiaodong Cui, 2023), (Martínez L, 2009) show linearithmic (O(N log N)) time complexity. Implement bin-packing informed by bounding box and accessibility metrics.
  - Advances in 3D path routing (Yang, 2016) show time complexity between O(N log N) and N^2. Implement 3D path routing of interconnects, informed by total interconnect length and accessibility metrics.
  - This proposed path will first do 3D bin packing of the components in the system architecture, then do 3D path planning of the interconnects.
  - Various approaches are available to generate a diverse set of component packings and path routings.
  - These packed and routed systems will then be sampled based on topological diversity, using either the Yamada polynomial, or other diversity metrics that are quicker to compute, e.g., the Alexander polynomial. (Colin Adams, 2020)
  - These diverse packed and routed systems will then be analyzed to find physically meaningful diversity w.r.t. the physics and sensitivity to it, e.g., as was demonstrated earlier within this Seedling, meaningful diversity w.r.t. thermal sources and components known to be sensitive to heat. This diversity selects for configurations that have different combinations of component locations w.r.t. other components and external regions that are sources and sinks for physical effects.
  - Path 2 is the path that the Task 1 team proposes to design and demonstrate improvements possible in scalability.

4.1.2 Co-optimization of Physics and Spatial Configuration Demonstrated

1) Optimized Geometry Corresponding to each Topology as shown in **Table 3**:

Table 3: Computational Profiling of Co-optimization

System Architecture Specification		
# of components:	14	
# of interconnects (wires, pipes, ducts):	21	
Computation Timing:	Seconds/iteration	% of iteration computation
Packing volume:	0.001	0.4%
Route Length:	0.001	0.4%
Collision detection:	0.070	26.1%
Gradient calculation:	0.197	73.2%
Total computation:	**0.270**	**100.0%**

- Achieved geometric optimization of spatial topologies, using collision detection to stay within the relevant cell (consumed only 26% of the geometric optimization computation, while gradient calculation consumed 73%).
- Used MDBD to represent the component geometries and used cylinders to represent the interconnects as piecewise-linear path routings with a given diameter (i.e., wires, pipes, ducts).
- Component-component collision detection involved MDBD sphere center point distance calculations and comparison with the corresponding spheres' radii. Component-interconnect collision detection was MDBD sphere center point/line-segment distance calculations and radii comparisons. Interconnect-interconnect collision detection was line-segment/line-segment distance calculations and radii comparisons.

- Identified an **additional technical challenge**:
  - The design space of geometric optimization of complex system packagings includes many local optima, because compact packagings are often geometrically isolated amidst a sea of infeasible packagings (due to tight packaging). These local minima correspond to separate basins of attraction and require multiple diverse optimization multi-start points to ensure finding the global optimum. Efficient identification of multiple, diverse 3D spatial layouts of a given spatial topology was developed and demonstrated in Task1.

- Demonstrated robust convergence of combined geometric and physics-based optimization for each topology provided, using collision detection to ensure that each geometric optimization solver stays within its own cell.
  - Geometric optimization, with components represented via Maximal Disjoint Ball Decomposition methods, was combined with physics-based thermal topology-optimization via projection methods. (Bhattacharyya, 2022) (leveraging software that is UIUC background IP from the NSF POETS Consortium's SPI2 Program).

2) Task2: Demonstrated End-to-End MDOP Workflow:

- Tested end-to-end prototype MDOP capability for both a simple problem, and for a more complex problem (the same simple and more complex problems that were tested for Task1, so together, Task1 and Task2 have tested the end-to-end prototype MDOP computational workflow.
- Demonstrated Co-Optimization as Part of MDOP Workflow (as shown in **Figure 26**).

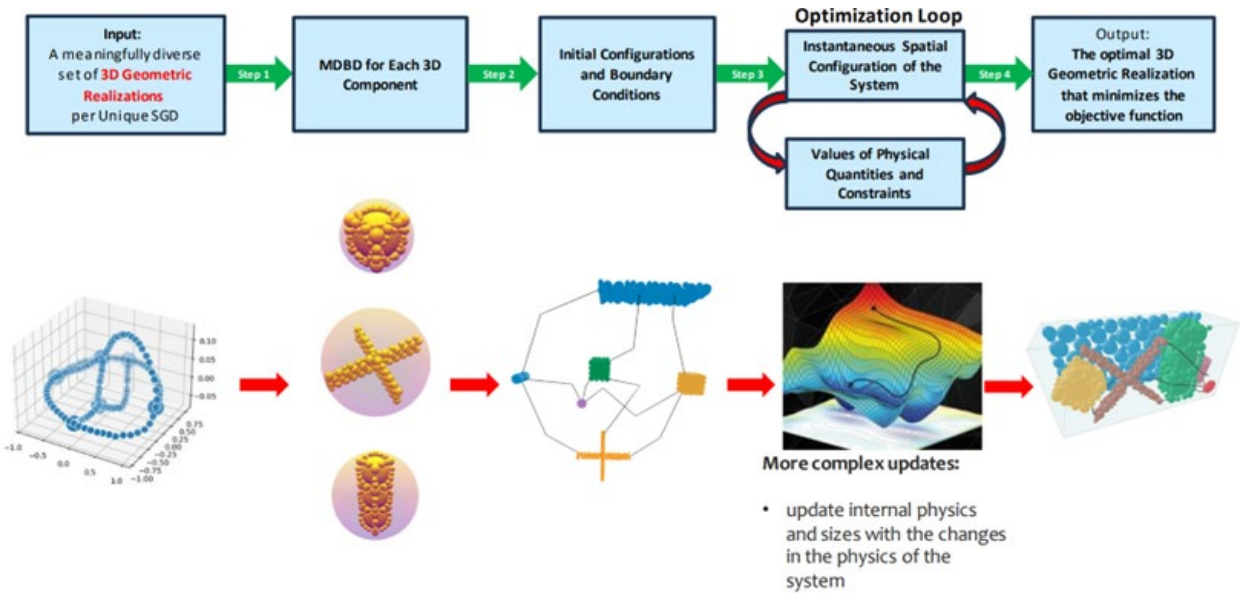

Figure 26: Computational Workflow of the MDOP Co-Optimization.

4.1.3 Co-optimization of Physics Spatial Configuration *and Accessibility* Demonstrated

- Demonstrated Task3 co-optimization including spatial configuration and accessibility, as shown in **Figure 27,** and including physics, spatial configuration and accessibility, as shown in **Figure 28**.

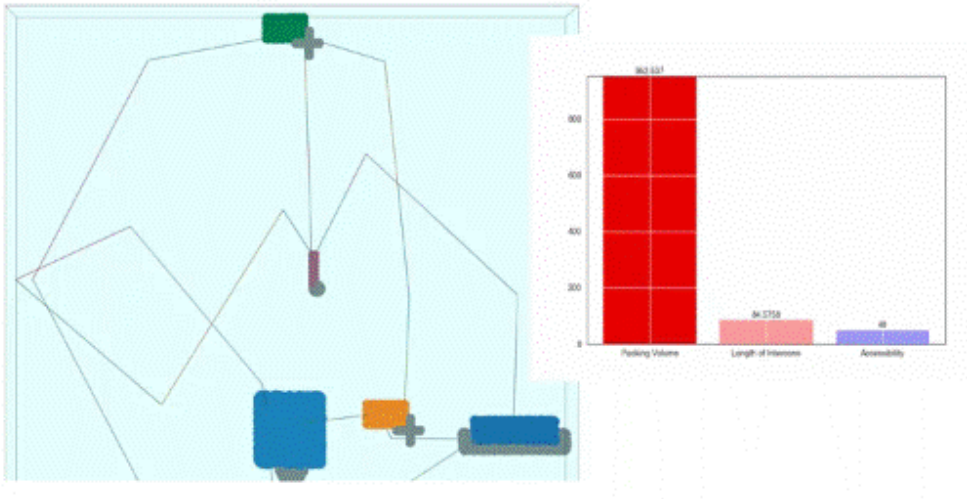

Figure 27: GIF of co-optimization of spatial configuration and spatial accessibility.

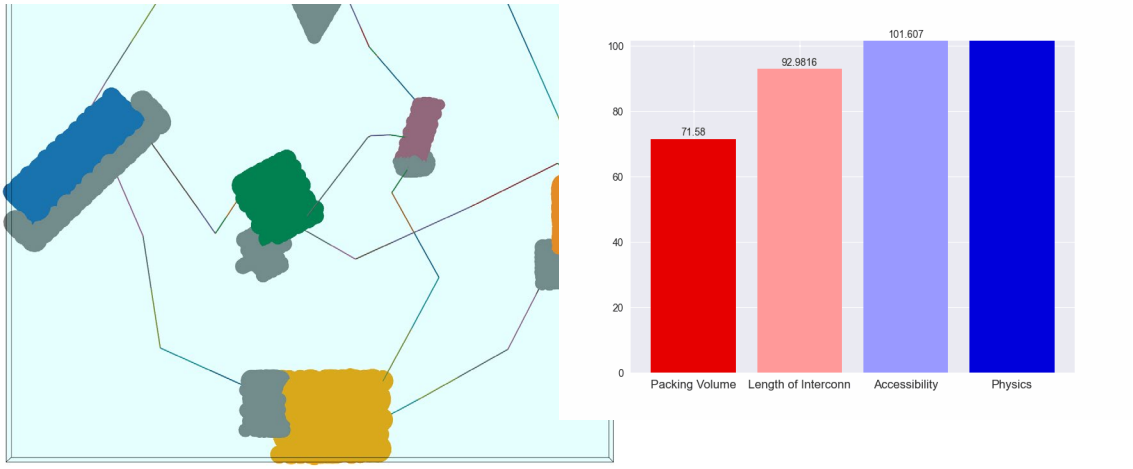

Figure 28: GIF of co-optimization of physics, spatial configuration, and spatial accessibility.

4.2 Validation Results for Computational Workflow Elements

The challenge problem highlighted the following key uncertainties for focused risk reduction:

- Tasks 1-3 treated the interconnect geometry as a set of straight segments between waypoints, which is fundamentally different from representing components by a set of spheres. Issues that might be raised by treating interconnects the same as components (representation with spheres) were uncertain. For the approach taken for modeling interconnect geometry, see **section 3.3.5.1 item 4**. For conclusions about interconnect modeling, see **section 5.1.4**.
- Tasks 1-3 did not enforce that the components and interconnects fit within a complex enclosure boundary, so, it was uncertain what sort of constraints and reasoning would be needed to enforce these constraints and enable optimal resizing and re-orientation of components, and redistribution of interconnect waypoints. For conclusions about how to implement spatial constraints, see **section 5.1.3**.
- Tasks 2 & 3 did not model components as capable of resizing driven by physics-based value metrics, managed by physics-based component sizing models, so it was uncertain how the co-optimization workflow would behave with resizing components, and physics-driven interconnect trajectories. For conclusions about resizing and re-orientation, see **section: 5.1.5**.
- Tasks 2 & 3 employed MDBD; however, because they did not model resizing components, it was uncertain how MDBD could function in a component-resizing optimization. For conclusions about MDBD applicability, see **section 5.1.2**.
- Tasks 2 & 3 employed different physics than was needed for the challenge problem. Further, RTX's DISCOVER physics models and computational infrastructure were agreed to be RTX background IP that would not be included in DARPA MDOP Seedling deliverables, nor would DISCOVER's continuous parametric optimization framework. So, it was uncertain how the DARPA MDOP Seedling deliverables would be functional for the challenge problem. It was decided that NASA's OpenMDAO optimization framework would be employed as software deliverables that could be provided to DARPA. The RTX physics would be implemented as a module that could be replaced with a non-proprietary drop-in replacement module, as a DARPA deliverable. For the architecture of this OpenMDAO integration with RTX physics models, and spatial configuration, see **section 3.3.5.1** item 1.

5.0 CONCLUSIONS

Results from the DARPA MDOP seedling offer the following conclusions:

- MDOP Methods
  - Topological Partitioning
  - MDBD
  - Enclosure Constraint(s)
  - Interconnect Constraint(s)
  - Combined Enclosure and Interconnect Constraint(s) and Interconnect Relocation
- MDOP's Potential Impact on Design of DoD Systems

5.1 MDOP Methods Assessment

The DARPA Seedling's Task4 Validation was designed to assess the MDOP Computational Workflow methods by attempting to apply them to a militarily relevant challenge problem – a pre-existing RTX proprietary UAV design was used as the context for this Task. The challenge problem intentionally included technical challenges that were different from the simple sets of shapes that the university subcontractors used; they were contracted to do fundamental research, with no tech data, and no proprietary data. Task4 Spiral2 included a duct with complex geometry, within which a heat exchanger(s) and inlet and outlet ducts must fit and be resized for the HX(s) to be as effective as possible (grow). The physics to size the heat exchanger is RTX proprietary background IP.

Note that the university subcontractors did not enable the components to be resized by the physics in their methods. As shown in **Figure 21**, NASA's OpenMDAO optimization framework was integrated in a modular fashion, so that the physics code *would* be included as a module that could be replaced by any other modular drop-in replacement when RTX's background IP was removed. The optimization problem has been fully flattened so that the OpenMDAO optimizer provides a design vector to each model (physics, spatial). The physics and spatial models are called independently; coupling is done entirely via constraints, other than the physics model passing the updated component and interconnect geometry to the spatial model for configuration.

5.1.1 Topological Partitioning Methods Assessment Conclusions

The TP method demonstrated within the MDOP Seedling scales up only far enough to handle systems with 14 components and 14 interconnects. Beyond that point, even though the infinite number of complex USTs in the complexity cones have been filtered out efficiently, the number of desirably simple spatial graphs rises exponentially, to the point that there are so many, that the probability of any two spatial graphs being unique is almost 100%.

So, the combinatorically growing number of likely USTs changes the computational need from checking for uniqueness, to sampling, a tiny subset of the number of simple USTs that the co-optimization's computing resources can handle – there is no way to co-optimize each UST, even using only one multi-start point per UST. **The most relevant sampling criteria** for this tiny subset of USTs that MDOP will be able to co-optimize, **is that they be as diverse as possible**, so that they each have a much higher probability of introducing useful topological novelty that can lead to high packaging value. While uniqueness says that at least one interconnect-pair crossing

(see **Figure 1**), must distinguish each sampled UST from all others in the sample, diversity goes much further. The number of crossings distinguishing each sampled UST from all others in an optimally diverse sample, must be as high as possible. (e.g., 10 or 20 crossings will differentiate each UST pair in the sample).

This need to sample the simple UST space for optimally diverse USTs impacts the multi-start approach. If trading computational capacity between optimizing twice in the same cell, vs. in two very diverse UST cells, the priority is clear – sample as many diverse USTs as possible and co-optimize with only one start point per UST cell (**no multi-start** beyond 14 components, 14 interconnects).

5.1.2 MDBD Assessment Conclusions

MDBD's sphere-based (center, radius) representation offers computational speed as well as other potential benefits. However, MDBD's disjoint representation does *not* support component resizing (other than 3D photo-scaling, equal in all 3 dimensions). Applying MDBD to an MDOP problem in which components resize, requires a new MDBD set of spheres to be identified each iteration, as the component is resized. This poses not only a significant computational cost during each co-optimization iteration, but more significantly, updating the MDBD set of spheres causes discontinuity in the distance computation, since the distance between objects is based on a different set of MDBD spheres at each co-optimization iteration.

For this discontinuity impact on the gradient, it is our validation conclusion that MDBD is incompatible with MDOP gradient-based optimization methods in problems where components can be resized during conceptual-design co-optimization. Instead, RTRC implemented a non-MDBD geometric representation, using a collection of spheres that overlap; the grid of their center points can be differentially stretched/compacted in 3D (NOT 3D photo scaling) which continuously varies their degree of overlap, but doesn't vary their shape (they're still spheres). This non-MDBD representation results in fast, continuous resizing of components. It can be inaccurate if there is a large change in aspect ratio, but this easily solvable with a denser grid in the relevant dimension, producing more spheres, and trades computational speed for accuracy. Versus MDBD, this method is not Maximal, so the volume is not efficiently consumed by the largest spheres possible. They are also not DISJOINT; they overlap – however, since MDOP is not doing volume calculations using these spheres, their overlap is irrelevant. It does share MDOP's property of representing the shape to an arbitrary degree of accuracy (the grid sizing and sphere sizing is continuously variable). While it is applicable for 2D, 3D, ..., it does not share MDBD's dimension-elevation property.

5.1.3 Enclosure Constraint Conclusions

The Task4 Validation team identified that they would need to develop a meaningful constraint, with suitable gradients to keep the components and interconnects within a complex enclosure. So, first, Spiral1 considered a simplified problem, a heat exchanger inside a box-shaped enclosure. To increase the effectiveness of the HX and reduce the pressure drop, the HX needs to grow its air-side surface area. Within the box enclosure, it needs to align itself diagonally to resize optimally.

In Figure 29, a GIF is shown of co-optimization runs with a single distance constraint between the HX component and the box enclosure boundary. It works poorly, because a single distance

constraint oversimplifies the relationship between the HX's grid of spheres and the box enclosure boundary. **Figure 30** shows that one constraint cannot capture this relationship well and enable reasoning about it.

In **Figure 31**, a GIF is shown of co-optimization runs with distance constraints between each sphere of the HX component and the box enclosure boundary. It works better, because the collection of constraints is better able to represent the relationships between the HX's grid of spheres and the box enclosure boundary. **Figure 32** shows how multiple constraints can capture this relationship better and enable reasoning about it.

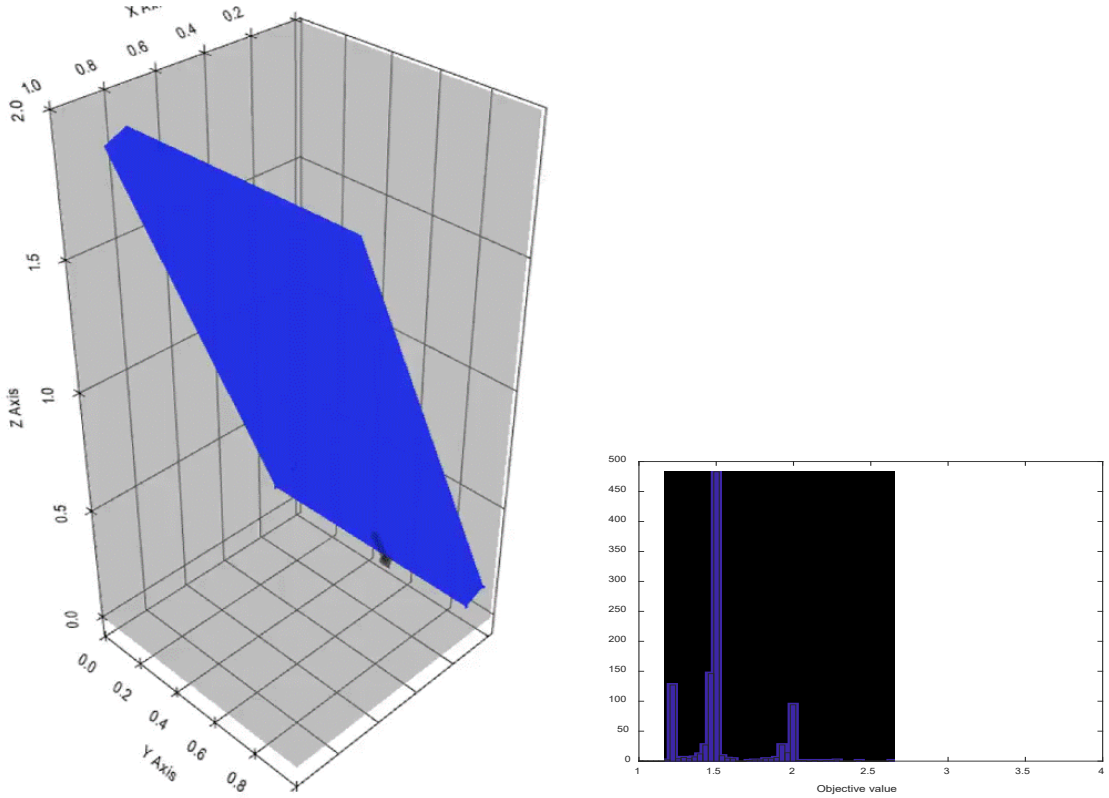

Figure 29: GIF (left) of Spiral1 co-optimization with single distance constraint shows poor stability. The histogram (right) shows that few optimizations found global optimum, while most got stuck on a local minimum.

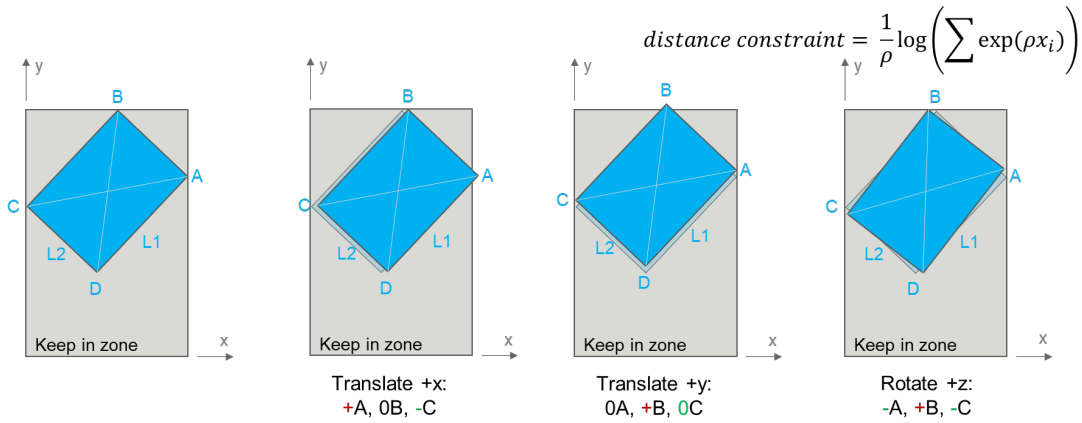

Figure 30: A single distance constraint is a poor representation of the component's spatial relationship to the enclosure boundary. In this case, the single constraint doesn't support reasoning because each of the component's corners has a different relationship with the enclosure boundary.

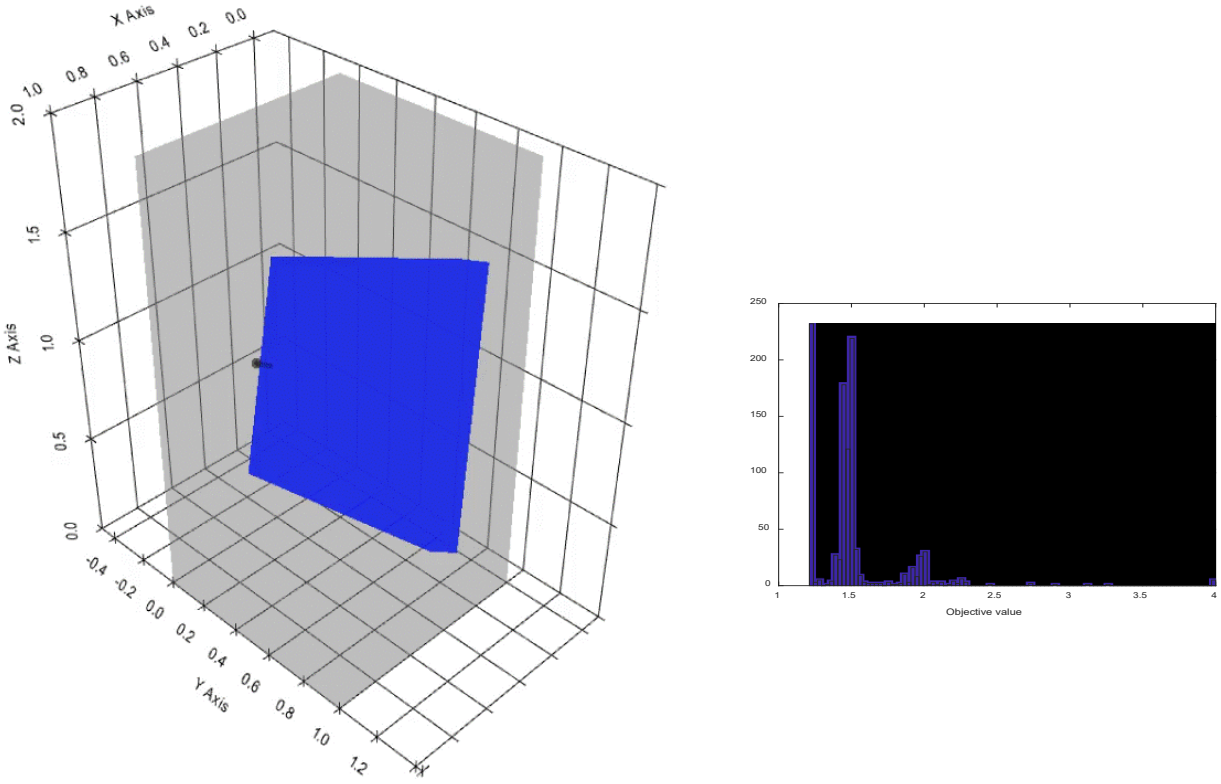

Figure 31: GIF (left) of Spiral1 co-optimization with distance constraints from each component sphere to enclosure boundary has better stability. Histogram (right) shows that some optimizations found the global optimum, while many got stuck on a local minimum.

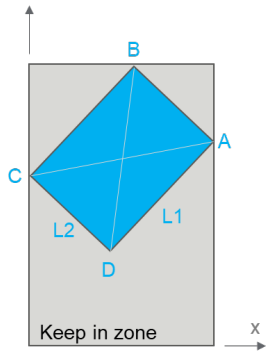

Constraint derivative (lower is better)

	Translate x +/-	Translate y +/-	Rotate z +/-	Scale L1 +/-	Scale L2 +/-
Min distance	+/0	+/+	+/+	+/-	+/-
Corner A	+/-	0/0	-/+	+/-	+/-
Corner B	0/0	+/-	+/-	+/-	+/-
Corner C	-/+	0/0	-/+	+/-	+/-
Corner D	0/0	-/+	-/+	+/-	-/+

From min distance: no feasible improvement indicated
From A, B, C: translate -y, rotate +z, scale +L1 and +L2

Figure 32: The distance constraint derivatives for each of these 3 component corners to the enclosure boundary do a better job of capturing and supporting reasoning about the component's spatial relationship with the enclosure boundary and how to increase component size while still fitting within the enclosure.

To sense the precise relationship between an arbitrary component shape and an arbitrarily complex enclosure boundary, the Task4 Validation team developed a reasoning implementation that uses both a Keep-In zone, inside the enclosure boundary, and a Keep-Out zone, just outside the enclosure boundary. The reasoning implementation establishes constraints that compare component spheres with both the Keep-In zone spheres and the Keep-Out zone spheres.

5.1.4 Interconnect Constraints

The Task4 Validation team then developed a similar constraint to enforce that interconnects fit within the enclosure, as well as a reasoning implementation to enable optimal relocation of interconnect waypoints to minimize pressure drop due to line losses and turning losses. **Figure 33**, shows a GIF of a co-optimization run validating this implementation, which achieves an optimal, smooth s-shaped curve.

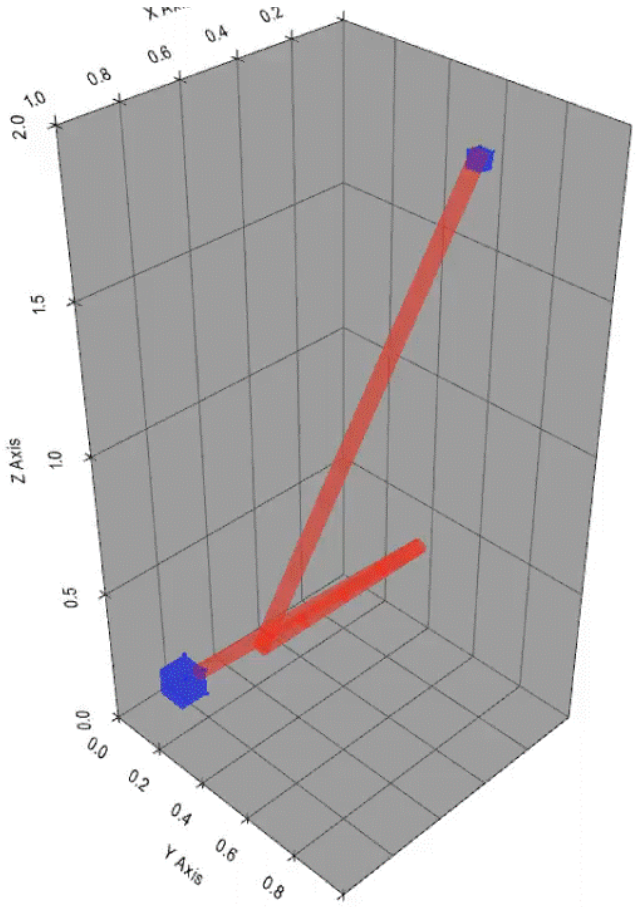

Figure 33: GIF of Spiral1.5 co-optimization of an interconnect and its optimum solution.

5.1.5 Combined Component and Interconnect Constraints and Waypoint Relocation

A co-optimization was run validating the combined constraints keeping the HX component and the inlet and outlet interconnects within the duct enclosure, while optimizing HX effectiveness and pressure drop. All components and interconnects end up inside the enclosure boundary. The HX appears to be optimally located, oriented, and sized.

5.1.6 MDOP's Potential Impact on Design of DoD Systems

5.1.6.1 The Need to Achieve Substantially More Aggressive DoD Requirements

The design of complex DoD systems by conventional design methods is limited in the functional density that can be achieved. This limit to the level of functional density (normalized for applicability from systems at the size of microelectronics to entire military ships) limits the system requirements that can be achieved to far less than those needed by the DoD. **Figure 34** shows a variety of DoD systems, the degree of functional density that can be achieved by conventional methods, the current limit of functional density that conventional design methods offer, and greater DoD requirements that could be met if the current limit of functional density could be improved substantially.

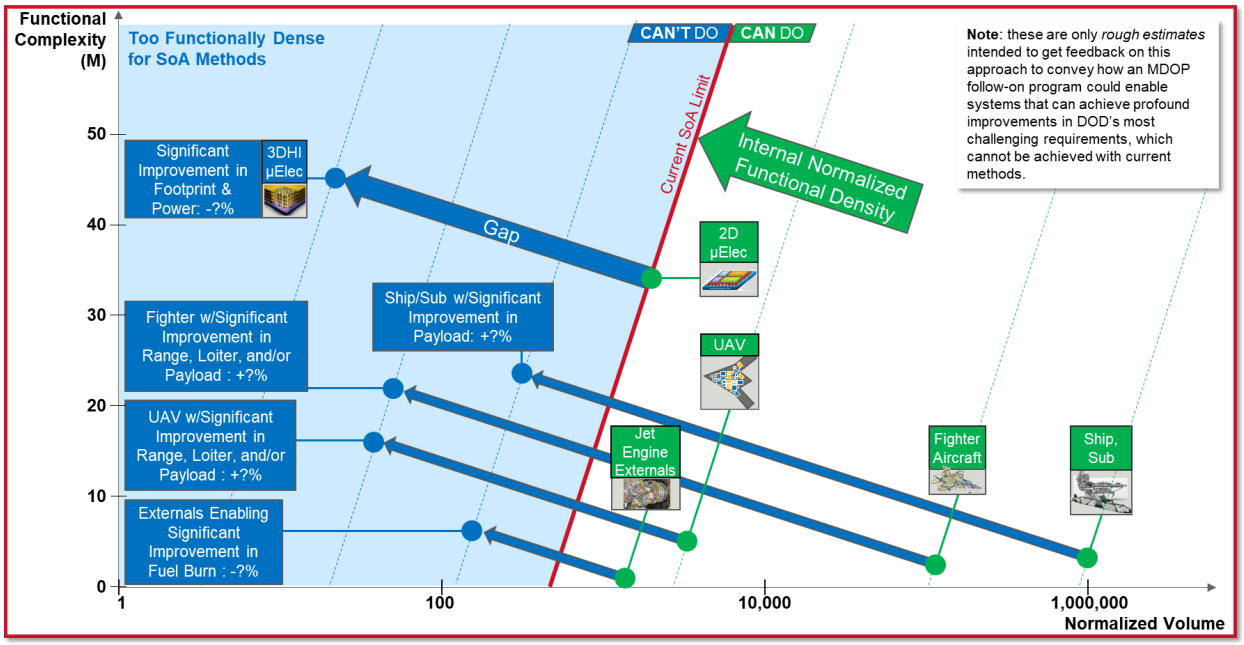

Figure 34: DoD systems that CAN'T be developed today due to packaging challenges.

The packaging challenges which DoD systems encounter stem from the late stage at which packaging is quantitatively considered. Conventional system design of Aerospace and Defense systems considers 3D spatial packaging late in detail design, long after the ideal performance has been optimized, design decisions have been made, and long-lead investments have been committed. When 3D spatial-packaging non-compliance is detected, late in detail design, the consequences to schedule and budget are severe. Even in compliant systems, the fielded value metrics often never achieve the ideal metrics forecasted by analyses that preceded 3D spatial packaging design.

If 3D spatial packaging could be co-optimized, during conceptual design, along with system physical considerations, the level of achievable system functional density could be substantially improved, resulting in substantially more aggressive, achievable DoD requirements.

Because 3D spatial packaging is done by computer-aided design (CAD) designers, late in detail design, without optimization or feedback on the consequences to value metrics, packaging expertise evolves slowly, centered around particular technologies and how to package them densely. New technologies lack this associated packaging expertise, so estimates of their functional density are low, and they do not compare favorably with conventional technologies, in conceptual design rough estimates, until this expertise evolves. This prevents the DoD from leveraging new technologies in an agile fashion as early as it could. Delaying adoption of the best new technologies jeopardizes military readiness and warfighter capabilities

3D spatial packaging is also a key to increasing fleet availability of DoD's current systems. The speed with which a system can be successfully maintained, diagnosed, repaired, or overhauled, and return to available status, depends directly on spatial accessibility. Spatial accessibility

drives maintenance duration & skill-level required, which directly drive fleet availability. Current design methods lack paradigms for modeling and simulation of spatial accessibility, during conceptual design. Spatial accessibility similarly drives DOD system life-cycle cost.

5.1.6.2 The Technical Challenge to Increase the Attainable Level of Functional Density

Substantially increasing the normalized functional density of DoD systems requires the ability to co-optimize physics-based system value metrics together with 3D spatial packaging, during conceptual design. That co-optimization requires fast computational assessment of well-designed spatial constraints, and value metrics that enable optimization to ensure that systems are driven toward physically realizable dense packaging, while still achieving other physics-based value metrics, such as performance, range, and loiter time.

Increasing the level of functional density achievable in design thus requires accelerating 3D spatial-packaging analysis by several orders of magnitude, so that it can be co-optimized during conceptual design. 3D spatial-packaging analysis must also address the full MDOP problem (see **section 2.1**). This amounts to the following DARPA-hard technical challenge:

An integrated, scalable solution is required to these sub-challenges, described in the following sections:

- Multi-region packaging
- Component resizing and reshaping
- Integrated interconnect complexity and flexibility
- Co-optimization of multi-physics, spatial proximity, and spatial accessibility
- Collision avoidance with enclosures and obstacles

The topic of creating an integrated scalable solution is the critical binding element in this technical challenge, which is addressed in a final section.

5.1.6.3 Multi-Region Packaging

As shown in **Figure 35**, this technical challenge is to extend recent advances in single-region packaging (in the DARPA MDOP Seedling) to address a wide range of DOD system-design problems in which subsystems are distributed across a variety of available volumes within different regions of a system (e.g., power distribution, distributed propulsion), minimizing the:

- weight,
- cost,
- losses (e.g., thermal, pressure drop, electrical) and
- accessibility impacts of cables, pipes, ducts interconnecting those regions.

More efficient multi-region packaging could also support multi-mode subsystem reconfigurability.

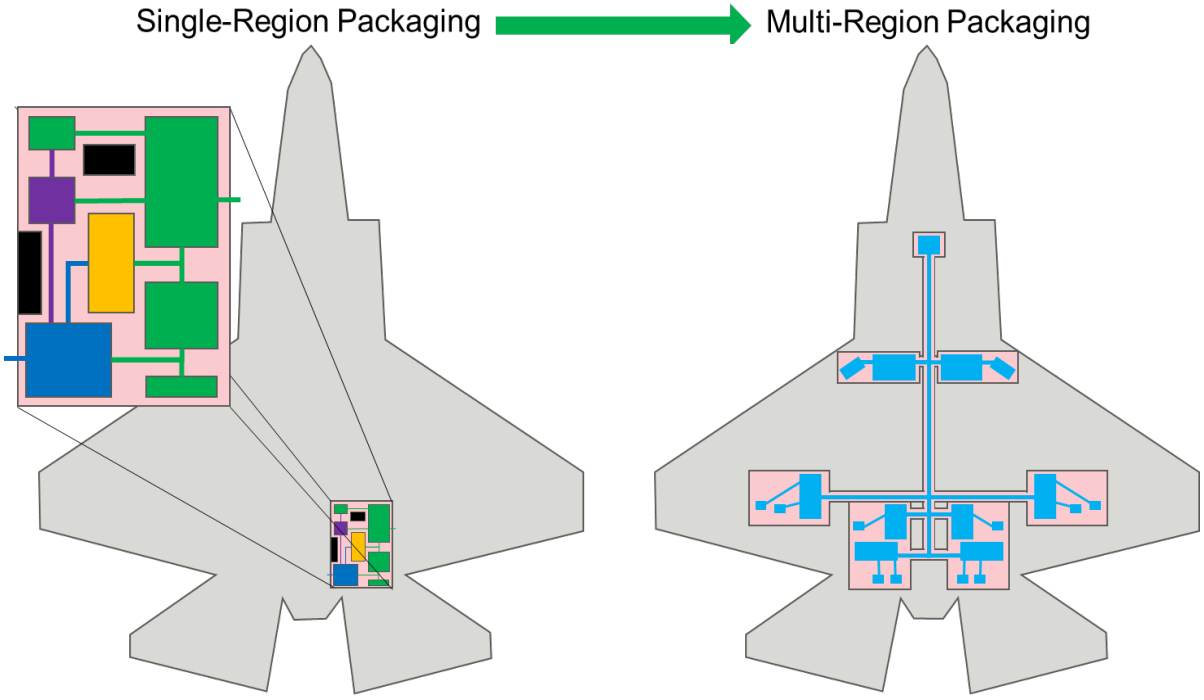

Figure 35: Multi-region packaging allocates components across a variety of available volumes in different regions within a system, and incurs weight, cost, losses, and accessibility impacts due to routing interconnects between those volumes.

5.1.6.4 Component Resizing and Reshaping

Extend recent advances (DARPA MDOP Seedling) in fixed-component packaging to address components (e.g., heat exchangers, fuel tanks) that can resize and/or reshape, during optimization, based on physics-based value metrics, as shown in **Figure 36**.

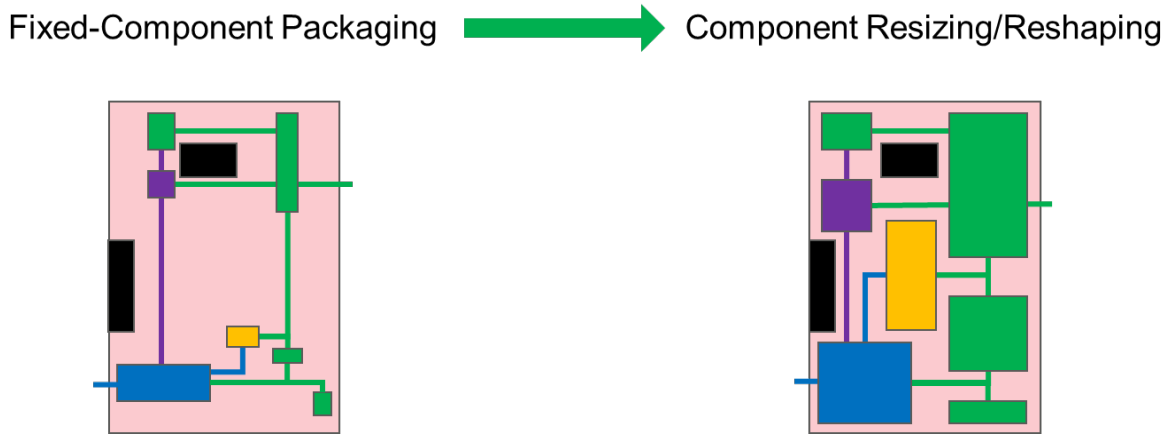

Figure 36: Components must be able to be resized/reshaped, during co-optimization, to optimize physics-based system value metrics.

5.1.6.5 Integrated Interconnect Complexity and Flexibility

As shown in **Figure 37**, a conceptual framework is needed to enable interconnects with these properties:

- interconnect shapes and sizes unlike those of wires or pipes, e.g.,
  - large ducts
  - with non-circular cross sections, and
  - cross sections that change along the length of the interconnect
- topologically complex multi-point interconnects with:
  - forks,
  - merges and
  - bundles (e.g., wire harnesses, ducting)
- direct component-to-component attachment, e.g.,
  - substrate-mounted components conveying structural, thermal and/or electrical loads the substrate
  - components directly connected to minimize losses
  - collocated multi-function subassemblies

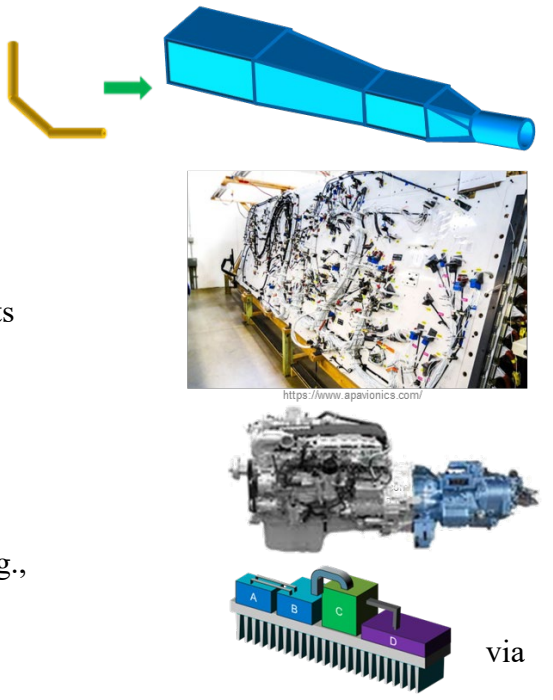

via

Figure 37: More-complex and flexible types of interconnects that must be addressed for applicability across a wide range of DoD systems.

5.1.6.6 Co-Optimization of Multi-Physics, Spatial Proximity, and Spatial Accessibility

This technical challenge was a focus of this DARPA MDOP Seedling. It must be included in the required integrated scalable solution that is the over-arching technical challenge.

5.1.6.7 Collision Avoidance with Enclosures and Obstacles

This technical challenge was a focus of this DARPA MDOP Seedling. It must be included in the required integrated scalable solution that is the over-arching technical challenge.

5.1.6.8 An Integrated Scalable Solution

As shown in **Figure 38**, an Integrated Scalable Solution is the over-arching technical challenge. It must extend recent breakthroughs in 3D spatial packaging by developing fast numerical, algorithmic and/or learning methods to enable rapid, computationally tractable solutions:

- Co-optimization of multi-physics, proximity, and accessibility,

- Collision Avoidance with enclosure & obstacles,
- Multi-Region Packaging,
- Component Resizing/Reshaping,
- Interconnect Complexity/Flexibility,
- Upfront in conceptual design, at scale.

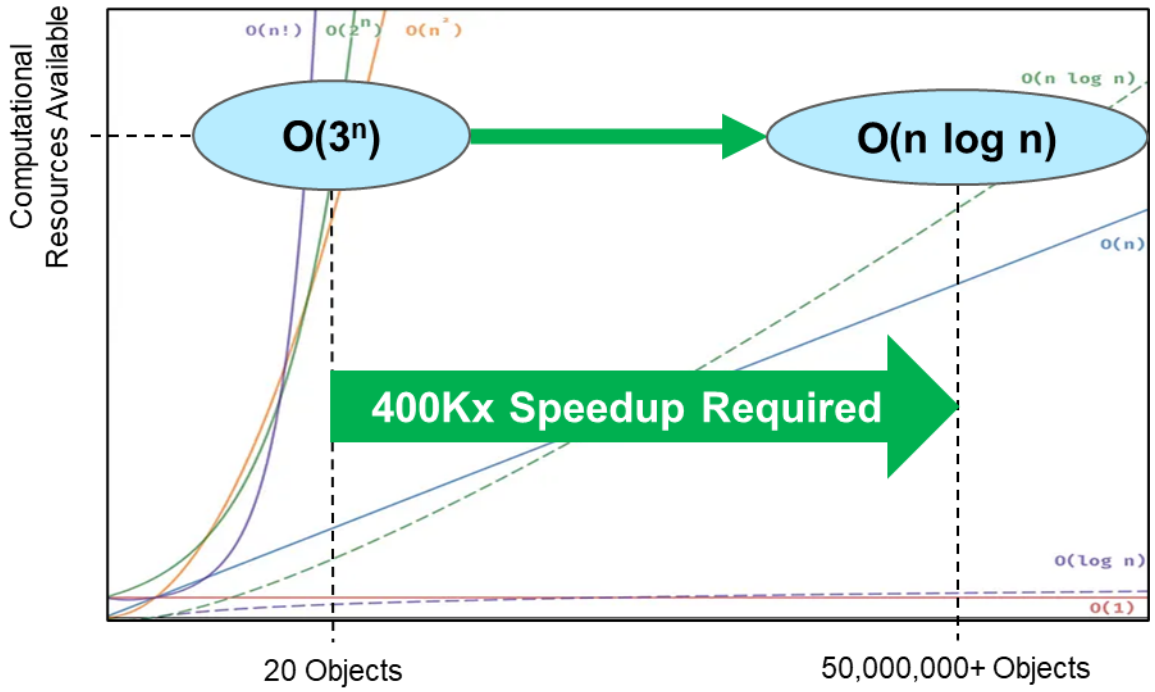

Figure 38: An integrated scalable solution is required to get MDOP from the O(3^n) curve onto the O(n log n) curve. This is needed to achieve 400,000 times speedup, which is required to achieve the most aggressive DoD requirements.

6.0 REFERENCES

Bhattacharyya, A. P. (2022). Simultaneous 3D Component Packing and Routing Optimization Using Geometric Projection. *AIAA SCITECH Forum* (pp. 2022-2096). San Diego: AIAA. doi:https://doi.org/10.2514/6.2022-2096

Colin Adams, E. F. (2020). Invariants of Spatial Graphs. In B. Mellor, *Encyclopedia of Knot Theory* (pp. 491-501). Theory CRC Press. doi:https://doi.org/10.1201/9781138298217-62

Dong, W. e. (2021). ASH: A Modern Framework for Parallel Spatial Hashing in 3D Perception. *Transactions on Pattern Analysis and Machine Intelligence, 45*, 5417-5435. doi:https://doi.org/10.48550/arXiv.2110.00511

Jiangce Chen, H. T. (2020). Maximal Disjoint Ball Decompositions for shape modeling and analysis. *Computer-Aided Design, 126*, 102850. doi:https://doi.org/10.1016/j.cad.2020.102850

Martínez L, A. R. (2009). PACKMOL: a package for building initial configurations for molecular dynamics simulations. *Journal of Computational Chemistry*, 2157-2164. doi:https://doi.org/10.1002/jcc.21224

Peddada, S. D. (2021). Systematic Enumeration and Identification of Unique Spatial Topologies of 3D Systems Using Spatial Graph Representations. *Proceedings of the ASME 2021 International Design Engineering Technical Conferences & Computers and Information in Engineering Conference IDETC/CIE2021.* virtual online: ASME. doi:https://doi.org/10.1115/DETC2021-66900

Peddada, S. R. (2022). Toward Holistic Design of Spatial Packaging of Interconnected Systems With Physical Interactions (SPI2). *ASME Journal of Mechanical Design*, 120801. doi:https://doi.org/10.1115/1.4055055

Qiaodong Cui, V. R. (2023). Dense, Interlocking-Free and Scalable Spectral Packing of Generic 3D Objects. *ACM Transactions on Graphics*, 1-14. doi:https://doi.org/10.1145/3592126

T. McMahon, S. T. (2014). Sampling-based motion planning with reachable volumes: Theoretical foundations. *IEEE International Conference on Robotics and Automation (ICRA)*, (pp. 6514-6521). Hong Kong, China. doi:https://doi.org/10.1109/ICRA.2014.6907820

Vesnin, A. a. (1996). *The Yamada polynomial for graphs knottedly embedded in a three dimensional space.* (Vychil. Sistemy ed., Vol. 155).

Yang, L. &. (2016). Survey of Robot 3D Path Planning Algorithms. *Journal of Control Science and Engineering*, 1-22. doi:https://doi.org/10.1155/2016/7426913

LIST OF SYMBOLS, ABBREVIATIONS, AND ACRONYMS

2D	Two-Dimensional
3D	Three-Dimensional
3DGR	3D Geometric Realization
3DHI	3D Heterogeneously Integrated
4D	Four-Dimensional
CAD	Computer-Aided Design
CPS	Cyber-Physical Systems
CPU	Central Processing Unit
DARPA	Defense Advanced Research Projects Agency
DOD	Department of Defense
EMI	Electromagnetic Interference
FDL	Force Directed Layout
FEA	Finite Element Analysis
FFT	Fast Fourier Transform
GIF	Graphics Interchange Format
GPU	Graphics Processing Unit
GR	Geometric Realization
HVAC	Heating, Ventilation, and Air Conditioning
HX	Heat Exchanger
I/O	Input/Output
IP	Intellectual Property
MDAO	Multi-Disciplinary Analysis & Optimization
MDBD	Maximal Disjoint Ball Decomposition
MDOP	Multi-Disciplinary Optimization for Packaging
NASA	National Aeronautics and Space Administration
NSF	National Science Foundation
OpenMDAO	NASA's Open-Source MDAO Framework
POETS	Power Optimization for Electro-Thermal Systems
RQ	Research Question
RTRC	Raytheon Technologies Research Center
RTX	Raytheon Technologies Corporation

SBMP	Sampling-Based Motion Planning
SG	Spatial Graph
SGD	Spatial Graph Diagram
SPI2	Spatial Packaging of Interconnected Systems with Physical Interactions
SWaP-C	Size, Weight, Power and Cost
TP	Topological Partitioning
UAV	Unmanned Aerial Vehicle
UConn	University of Connecticut
UIUC	University of Illinois Urbana-Champaign
UST	Unique Spatial Topology
W.R.T.	With Respect To
YP	Yamada Polynomial